



# Detailed Mapping of the Spin Ghar Active Fault System in Eastern Afghanistan Based on Satellite Image Interpretation

Zakeria Shnizai <sup>\*1,2</sup>, Richard Walker <sup>2</sup>

<sup>1</sup>St John's College, University of Oxford, St Giles', Oxford OX1 3JP, UK | <sup>2</sup>Department of Earth Sciences, University of Oxford, South Parks Road, Oxford OX1 3AN, UK

**Abstract** The Spin Ghar fault system is one of the major active structures in northeastern Afghanistan, stretching ~130 km east-west along the Spin Ghar Mountains in the Jalalabad Basin. The fault system includes a group of strike-slip and oblique-slip thrust fault strands only 25 km from Jalalabad City. However, there is no existing detailed map of the fault traces, which is essential for mitigating seismic hazard from future seismicity. We therefore studied the fault-related geomorphology based on the interpretation of satellite images and shaded-relief topography. To identify exposed lithologies within the area we used true colour and false colour composite (FCC), band rationing and principal component analysis (PCA) on multispectral imagery. The Spin Ghar fault system is marked by both continuous and discontinuous linear and arcuate fault scarps developed in piedmont alluvium and along the Spin Ghar Mountain front. We also recognised scarps cutting bedrock terrain. Several deformed surfaces of Neogene-Quaternary age are observed along the fault strands in the Jalalabad Basin. The basin is also traversed by a series of east-west arcuate folds that suggest the area is undergoing south-north compression. The Quaternary faulting and seismicity demonstrate the kinematics of faulting in eastern Afghanistan. Our observations suggest that the east-west-trending right-lateral strike-slip and oblique-slip thrust faults are active and are important components of the seismic hazard in the eastern Afghanistan.

Executive Editor:  
**Robin Lacassin**  
Associate Editor:  
**Hongdan Deng**  
Technical Editor:  
**Mohamed Gouiza**

Reviewers:  
**M.-L. Chevalier**  
**J. Van der Woerd**

Submitted:  
**23 May 2023**  
Accepted:  
**5 March 2024**  
Published:  
**17 April 2024**

## 1 Introduction

Afghanistan is a land of mountains and desert plains situated within the Alpine-Himalayan orogenic belt, and is one of the most seismically active intracontinental regions in the world. Tectonic movements have related to India-Eurasia convergence caused the rock sequences to become folded, faulted, and uplifted, creating the highest mountain ranges (*Dhakal, 2015; Shnizai et al., 2024*) (Figure 1). Between 1900 and 2022, more than 40 earthquakes with a magnitude of Mw 7.0 or greater were recorded within Afghanistan and the surrounding region (*Dewey, 2006; Ekström et al., 2012; ISC-EHB, 2023; USGS, 2023*). Thus, the country is very prone to seismic hazards.

The greatest seismic hazard in Afghanistan is in the east and northeast parts of the country. The active fault systems in these regions are largely controlled by Indian-Eurasian convergence. Active faults in eastern Afghanistan have uplifted the Hindu Kush and Pamir Mountains Ranges, as well as forming wide belts of low-elevation mountainous terrain

that are intertwined with fault-bounded low-relief sedimentary basins (*Shnizai et al., 2022*) (Figure 1a). One of the major faults in eastern Afghanistan is the Spin Ghar fault system that consists of a group of strike-slip and oblique-slip fault strands, showing clear evidence of active faulting in Quaternary basin deposits (Figure 1a-b).

The Spin Ghar fault stretches east-west along the border of the Jalalabad Basin and the Spin Ghar Mountains (Figure 2). The Jalalabad Basin is a large eastward-draining basin that is structurally controlled with a semi-arid subtropical steppe climate (Figure 1b). In the basin, Jalalabad city is the fourth most populated city in Afghanistan, covering an area of 122 square kilometres (Figure 2). According to the findings of the State of Afghan Cities Program, Jalalabad City's population is estimated to be between 296,895 and 356,274 people (*MUDA, 2015*). In this earthquake-prone area, many buildings and houses are constructed without adhering to appropriate standards or taking into account active faults. The houses are made of mud blocks, held together by mud, with thick flat roofs supported by wooden beams and mud block

\*✉ [zakeriashnizai@gmail.com](mailto:zakeriashnizai@gmail.com)

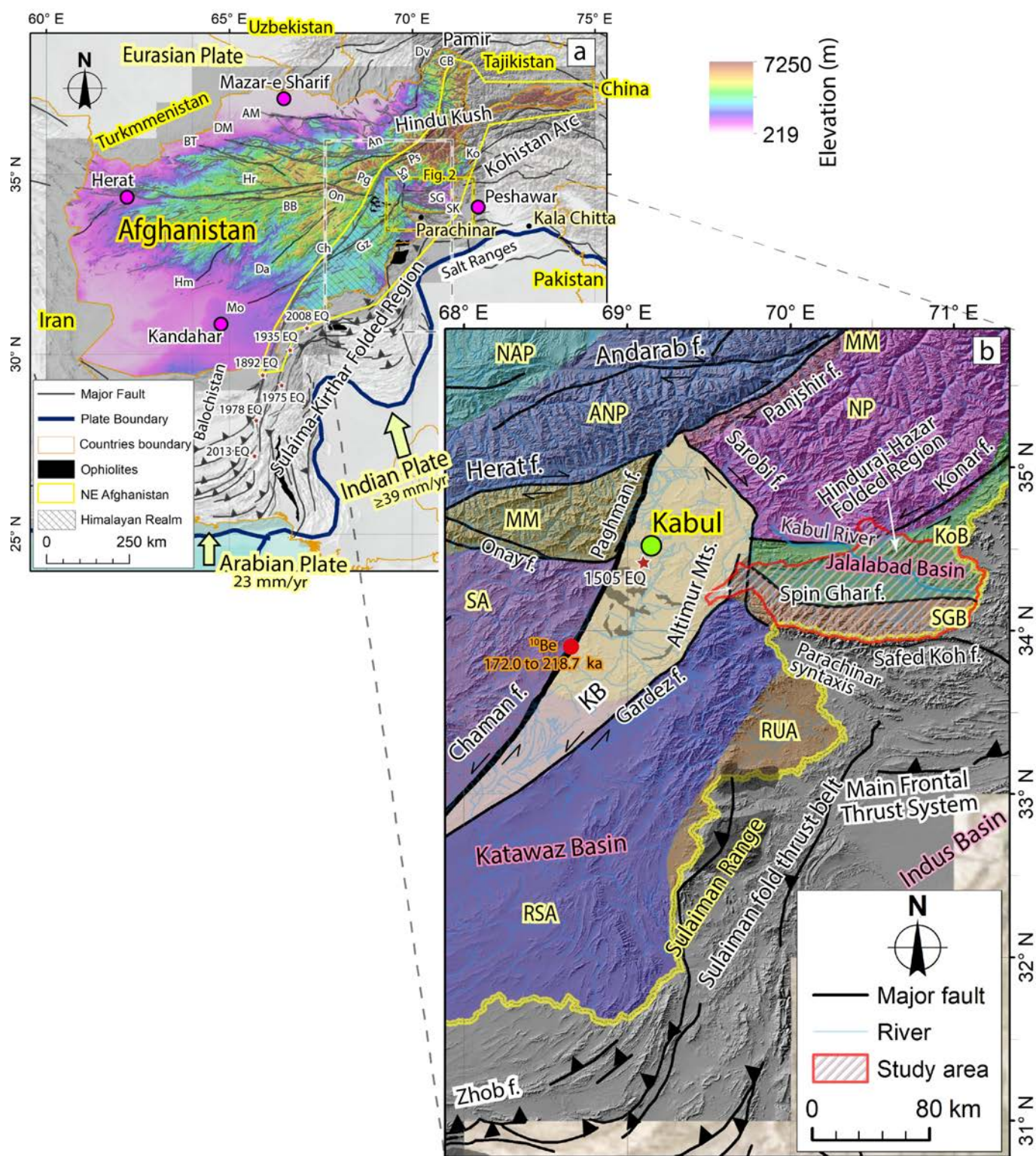


**Figure 1 – a)** Tectonic map of Afghanistan and the surrounding region showing the plate boundary and major faults. Abbreviation of faults: AM, Alburz Mormul; An, Andarab; BB, Bande Bayan; BT, Bande Turkestan; Ch, Chaman; CB, Central Badakhshan; Da, Darafshan; Dv, Darvaz; Dm, Dosi Mirza-Valang; Gz, Gardez; Hr, Herat; Hm, Helmand; Ko, Konar; Mo, Mokur; On, Onay; Pg, Paghman; Ps, Panjshir; Sa, Sarobi; SG, Spin Ghar; SK, Safed Koh. Yellow arrows show relative plate motion directions of the Arabian and Indian plates with respect to the Eurasian plate. The yellow polygon shows location of east-northeast Afghanistan. Afghanistan sits at the meeting point of the Indian, Eurasian, and Arabian plates, resulting in a unique geological environment with diverse features and seismic activity. The Himalayan Realm were formed when the Indian Plate collided with the Eurasian Plate and caused a shift in the geodynamic setting of south-eastern Afghanistan including the Sulaiman-Kirthar Folded Region and Kohistan Arc. **b)** Sketch map of tectonic zones of eastern Afghanistan (modified from *Abdullah et al.*, 2008). Abbreviation of blocks: ANP, Afghanistan-North Pamir; KB, Kabul Block; KoB, Konar Block or Henduraj-Hazar Folded Region; MM, Median Masses (Region of Middle Kimmerian); NAP, North Afghanistan Platform; NP, Nuristan-Pamir; RSA, Relatively Subsidized Area; RUA, Relatively Uplifted Area; SA, South Afghanistan or Accreted Terrain (Regions of Alpine Folding); SGB, Spin Ghar Block. The red polygon shows Location of the Jalalabad Basin.



walls. These structures are not reinforced against horizontal shaking, thus moderate to high-magnitude earthquake could lead to widespread collapse and numerous casualties. The Jalalabad basin forms the major part of eastern Afghanistan and extends to the border with Khyber-Pakhtunkhwa, with topography and geology controlled by active tectonics (Figures 1a, 2). The fault strands have a visible physiographic signature on satellite images. However, the active faults have not been studied in detail. Therefore, detailed mapping of the active faults is required to aid their characterisation and to evaluate their potential for generating earthquakes.

The main purpose of this paper is to understand the active tectonics of eastern Afghanistan, particularly in the Jalalabad Basin and northern front of the Spin Ghar Mountains, by interpreting the tectonic geomorphology of the Spin Ghar fault system. The study focuses on understanding the active deformation of the study area by interpreting the tectonic geomorphology of the study area. We map active structures based on the interpretation of 3D anaglyph images, constructed from the Shuttle Radar Topography Mission (SRTM) digital elevation model (DEM) with 30 m resolution, combined with an interpretation of Landsat 8 satellite imagery for lithological and tectonic mapping. We describe the tectono-geomorphic features along the Spin Ghar fault zone in detail and explain the relationship between various geological structures. Our detailed mapping leads to recognition of numerous fault scarps cutting bedrock terrain and surficial deposits that clearly display morphological evidence of recent activity.

## 2 Tectonic Setting

Afghanistan lies within the Alpine-Himalayan orogenic belt, developed in response to the collision between the Arabian, Indian and Eurasian plates from approximately 55 million years ago to present-day (Late Palaeogene to Holocene) (Aitchison *et al.*, 2007; Quittmeyer and Jacob, 1979; Treloar and Izatt, 1993). Deformation is inferred to have begun in the Oligocene onset of Himalayan orogenic movements inferred from a regional unconformity (Shnizai, 2020a,b; Siehl, 2017) (Figure 1a). Continental collision and strike-slip faulting has caused thickening uplift of the continental crust in the eastern Afghanistan from the presence of a regional unconformity. Surface uplift has led to development of a regional highland, inverting the prior tectonic relief (Shnizai *et al.*, 2024, 2022; Tapponnier *et al.*, 1981). Shortening between India and Eurasia continues on structures such as the thrust faults within Sulaiman-Kirthar Folded Region and Salt Ranges (Shnizai *et al.*, 2022), which also contain several shear zones and faults trending north-northeast causing horizontal movements along strike-slip faults (Tapponnier *et al.*, 1981) (Figure 1a-b).

Moderate to large magnitude earthquakes are common in the country due to the active deformation. East and north-eastern Afghanistan is one of the most seismically active zones, with more crustal earthquakes than any other region (Ambraseys and Bilham, 2003; Dewey, 2006; Ruleman *et al.*, 2007; Shnizai, 2020a; Wheeler *et al.*, 2005) (Figure 2). Eastern and north-eastern Afghanistan are cut by large active and potentially active faults such as the Chaman, Gardez, Paghman, Panjshir, Central Badakhshan, Sarobi, Sping Ghar and Konar faults (Figure 1a). Within this zone, one of the prominent structures is the Chaman fault, which is approximately 860 km long, and separates the rapidly deforming eastern area from central and western Afghanistan (Shnizai, 2020a; Shnizai *et al.*, 2020) (Figure 1a-b). The Chaman fault extends much of the distance from the Makran coast of Pakistan to the Hindu Kush in north-eastern Afghanistan (e.g., Szeliga *et al.*, 2012; Shnizai *et al.*, 2024, 2022; Shnizai and Tsutsumi, 2020; Shroder *et al.*, 2022; Ul-Hadi *et al.*, 2013) (Figure 1a). This fault is a significant geological feature located in Afghanistan and Pakistan, which has led to tectonic activity and creation of various geologic structures in the region. The Chaman fault is a left-lateral strike-slip fault accommodating tectonic deformation generated by the plate collision between Indian and Eurasian plates. Several studies have estimated the left-lateral slip rate of the Chaman fault to range from 5-35 mm/yr with overdue reduction from south to north (e.g., Beun *et al.*, 1979; Crupa *et al.*, 2017; Dalaison *et al.*, 2021; Lawrence *et al.*, 1992; Shnizai, 2020b; Shnizai *et al.*, 2024, 2020; Szeliga *et al.*, 2012; Ul-Hadi *et al.*, 2013). Based on the displacement of four geologic features with age from 25-20 Ma, Lawrence *et al.* (1992) estimated a slip rate of 19-24 mm/yr along the Chaman fault. According to Mohadjer *et al.* (2010) measurements based on GPS over a period of 7 years showed a slip rate of  $18 \pm 1$  mm/yr. According to studies by Crupa *et al.* (2017), the fault at latitude  $31.0^\circ$  N and  $31.96^\circ$  N has a slip rate of 8 mm/yr based on InSAR data. Dalaison *et al.* (2021) stated that a seismic slip along the Chaman fault is 12 mm/yr with three large distinct aseismic sections. Based on beryllium-10 cosmogenic dating of alluvial fans offset by the northern Chaman fault, Shnizai *et al.* (2020) found that the Chaman fault accommodates at 3.5-4.5 mm/yr of left-lateral strike-slip near Kabul, while in the southern Afghanistan in Baluchistan the slip rate is 33 mm/yr as estimated by Ul-Hadi *et al.* (2013). Throughout history, movement of the Chaman fault has caused moderate to large magnitude earthquakes in the region. On July 5 or 6, 1505 a significant earthquake occurred in Kabul causing widespread damage and casualties in Kabul and the surrounding regions. That earthquake had a magnitude of 7.2, and was felt as far as Delhi, India (Quittmeyer and Jacob, 1979). The Chaman fault system has been the site of several other notable earthquakes, including a 6.5 magnitude earthquake near Chaman in 1892, a 7.7 magnitude in Quetta 1935, 6.7 magnitude earthquake in 1975,

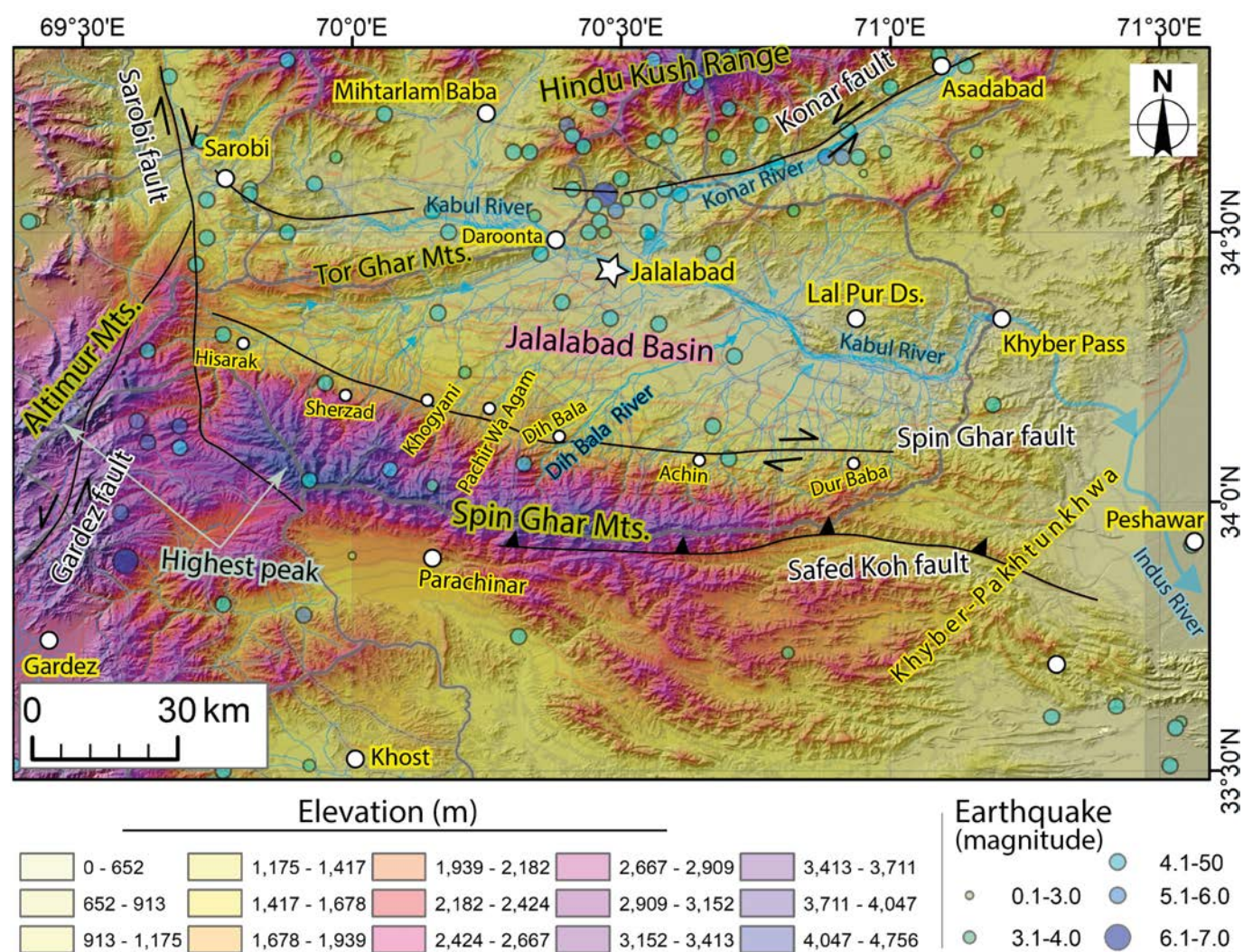


**Figure 2** – Map of the eastern Afghanistan and associated seismicity. Crustal seismic activity in Afghanistan is caused by the most significant active faults. Geomorphologically, the study area can be divided into two parts: an uplifted region known as Spin Ghar Mountains and the downthrown depression called Jalalabad Basin. The map shows the location of Jalalabad City with a white star, and small districts or cities with white circles. This map combines various datasets such as DEMs, shaded relief maps, river network, and provincial shapefiles to provide accurate elevation information and realistic landscape visualization. The map location is shown in Figure 1a.

a 6.1 magnitude earthquake in Nushki 1978, a 7.7 magnitude earthquake in Baluchistan in 2013, and a 6.4 magnitude earthquake in Ziarat district of Baluchistan in 2088 (e.g., *Ambraseys and Bilham, 2003, 2014; Quittmeyer and Jacob, 1979; Shareq, 1993, 1981; Wheeler et al., 2005; Yeats et al., 1979*) (Figure 1a).

The Spin Ghar fault is sited near the northern end of the Chaman fault where the fault breaks into a number of segments that separate individual forms of basins. The Spin Ghar fault is one of the major active structures in eastern Afghanistan, which separates the Konar Block from the Spin Ghar Block (Figures 1b, 2). The Spin Ghar fault trace is linear, but discontinuous (*Shnizai, 2020a,b*). The Konar Block occupies a range of small hills along the right and left sides of the Kabul River (Figure 1b). South of the Kabul River, the Spin Ghar Block covers most of the Spin Ghar Ranges, which are part of the Sulaiman-Kirthar Folded Region (e.g., *Abdullah et al.,*

2008; *Shnizai et al., 2024, 2022*) (Figure 1a). The Spin Ghar Block lies within the limits of the Spin Ghar Mountains in the south-eastern part of Afghanistan. This block covers a region about 140 km long and 30 km wide and stands higher than the surrounding terrain as a horst-type uplift (Figure 1a-b). The block is bounded to the north by the Konar Block along the Spin Ghar fault, and to the south by the Safed Koh fault (Figure 1b). The Katawaz Basin and the Sarobi right-lateral strike-slip fault border the Spin Ghar Block's western side. The Sarobi fault separates the Spin Ghar Block from the Kabul Block, and is one of the most seismically active regions in Afghanistan (Figure 1b).

### 3 Data and Methods

We aim to enhance and differentiate geological units and to interpret deformed geomorphic features, and classify the activity of faults in the Jalalabad



Basin and along the Spin Ghar Mountains. We use and combine several different remote sensing data sets to map the Spin Ghar fault system within an area that has received little attention (Figures 1b, 2). The main focus is on the Jalalabad Basin, the northern slope of the Spin Ghar Mountain, where we have observed recent deformation of right-lateral and dip-slip faulting. We use SRTM DEMs and Landsat 8 OLI (Operational Land Imager) and TIRS (Thermal Infrared Sensor) data (available at the <https://earthexplorer.usgs.gov>). SRTM DEM images with 30 m resolution were processed using SimpleDEMViewer software (<http://www.jizoh.jp>) to create three-dimension anaglyph images, which were interpreted and viewed through red and cyan glasses. The anaglyph image creates a 3D simulation using both the shaded relief and the DEM data with overlain and spatially offset of red cyan layers that we were able to visualize in 3D and observe the expression of geomorphology. Wearing the red and cyan glasses, the red channel (band) of the image is visible to the left eye, and the blue channel is visible to the right eye, allowing the wearer to perceive depth and to visualise the DEM in 3D. This allows for the identification of tectonic geomorphic features with great detail. Furthermore, we used shaded-relief, slope, and topographic maps to analyse the landscape and to determine if there are any active faults. We also made use of high-resolution optical satellite imagery within the ESRI (Environmental Systems Research Institute) and Google Earth base maps (<https://earth.google.com>). Based on our analysis, we created a map of the active and presumed active faults using ArcMap and Global Mapper software.

Geomorphic features such as stream offsets, beheaded channels, displaced geomorphic surfaces, fault scarps, linear depressions and pressure ridges were identified and mapped from the data sources as described above. These features were characterized based on their continuity and expression on the surface with vertical and horizontal offsets. We focus on the apparently young offset landforms and sediments, but in places where young deposits are scarce in steep mountains area, the interpretation was based on the presence of prominent and continuous bedrock escarpments. The images also help us to determine the geological structure, relative age, systematic offset, and geological and geomorphological observations about the Spin Ghar fault strands. Generally, the active faults are divided into active and presumed active faults based on the geomorphic criteria commonly used for active faulting to understand their behaviour (e.g., *Shnizai, 2020a; Shnizai and Tsutsumi, 2020*).

## 4 Results

### 4.1 Geological Mapping

#### 4.1.1 Landsat-8 Data Interpretation

Landsat 8 OLI images were processed to enhance geological features along the Spin Ghar Mountains and the Jalalabad Basin (Table 1; Figure 3a). Table 1 displays the band characteristics, including the number of bands, subsystem, spectral range, ground resolution, and swath width. Selected band combinations including false colour composite (FCC), band ratios, and principle component analysis (PCA) were effective in emphasizing the faults and differentiating rock types (Figures 3, 4). Spectrally, the visible and Near Infrared (NIR) bands highlight the presence of iron oxide minerals, while the Shortwave Infrared (SWIR) spectrum is specific for the detection of CO<sub>3</sub>, Al-OH, SO<sub>4</sub>, and NH<sub>4</sub>-bearing minerals. Also, SWIR (1.560-1.66 µm) is used to discriminate the moisture content of soil and vegetation. The thermal infrared sensor (TIR) can map silicate and carbonate minerals (*Adiri et al., 2020; Azizi et al., 2010; Grebby et al., 2014; Hashim et al., 2013*).

We built RGB (Red, Green and Blue) colour composites from visible and infrared bands 7-5-2 and 4-3-2, which shows high variation between rock types and vegetation cover (Figure 3a-b). Band rationing and supervised classification was also used to help sharpen images, remove the effects of shadowing, and to magnify differences between different types of materials on the earth surface (e.g., *Abdelaziz et al., 2018; Inzana et al., 2003; Yang et al., 2008*) (Figures 3c, 4a-b). The band ratio method is useful in highlighting some geological structures and rocks that cannot be seen in the raw bands such as in Figure 3a-b. Principal component analysis (PCA) was performed to produce enhanced contrast images in a false colour composite, with principal component outputs applied as RGB channels (e.g., *Ghrefat et al., 2021*). The PCA (pc1, pc3, pc5) provides the best discrimination between different rock types to construct a geological map of the Jalalabad Basin (Figure 4c). The PCA composite images make the best use of colour content in the visualization, when composites to false colour and ratio composites, as shown in Figures 3a-c and 4a-b.

We then used a supervised classification for all previous band combinations, band ratio and PCA to better discriminate the rock units in the area (Figures 3, 4). The accuracy of the Landsat 8 data assessment was verified using older and lower resolution geological maps of the study area (e.g., *Abdullah et al., 2008; Afghanistan Geological Survey, 1996; Doebrich et al., 2006*) (Figure 5).

#### 4.1.2 Geology of the Study Area

Various geological and geomorphological units are exposed in the study area. The various earth surface materials have distinct spectral signatures

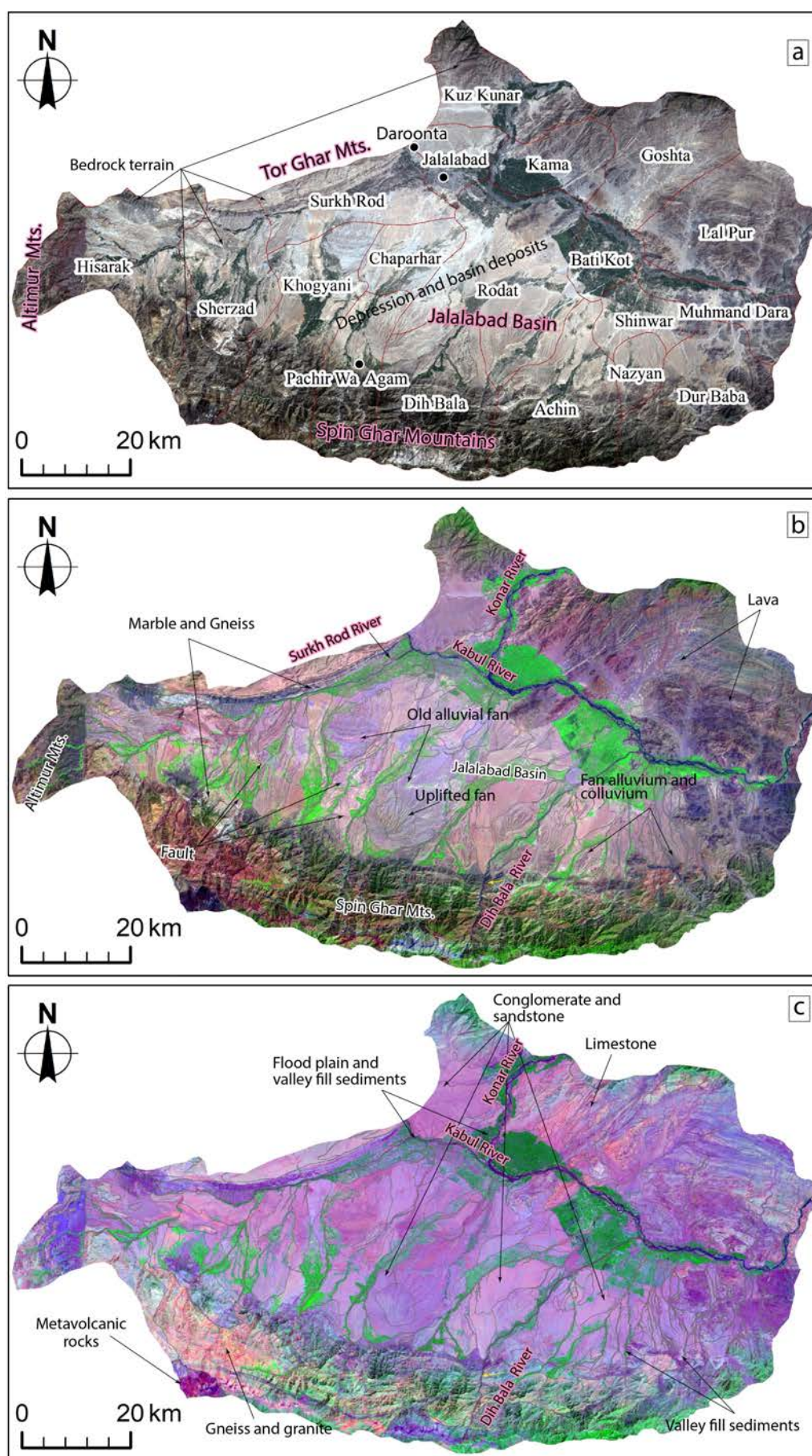


**Figure 3 – a)** Landsat 8 true colour composite image (bands 4, 3, and 2) showing geological structure and different rock types in the Jalalabad Basin. **b)** The false colour composite of band 7 (SWIR-2), band 5 (NIR) and band 2 (blue). Bedrock and sedimentary rocks are characterised by different colours. **c)** Band ratio image of bands 7/5-6/3-4/3. The band characteristics such as band number, subsystem, spectral range, and ground resolution and swath width are shown in Table 1.



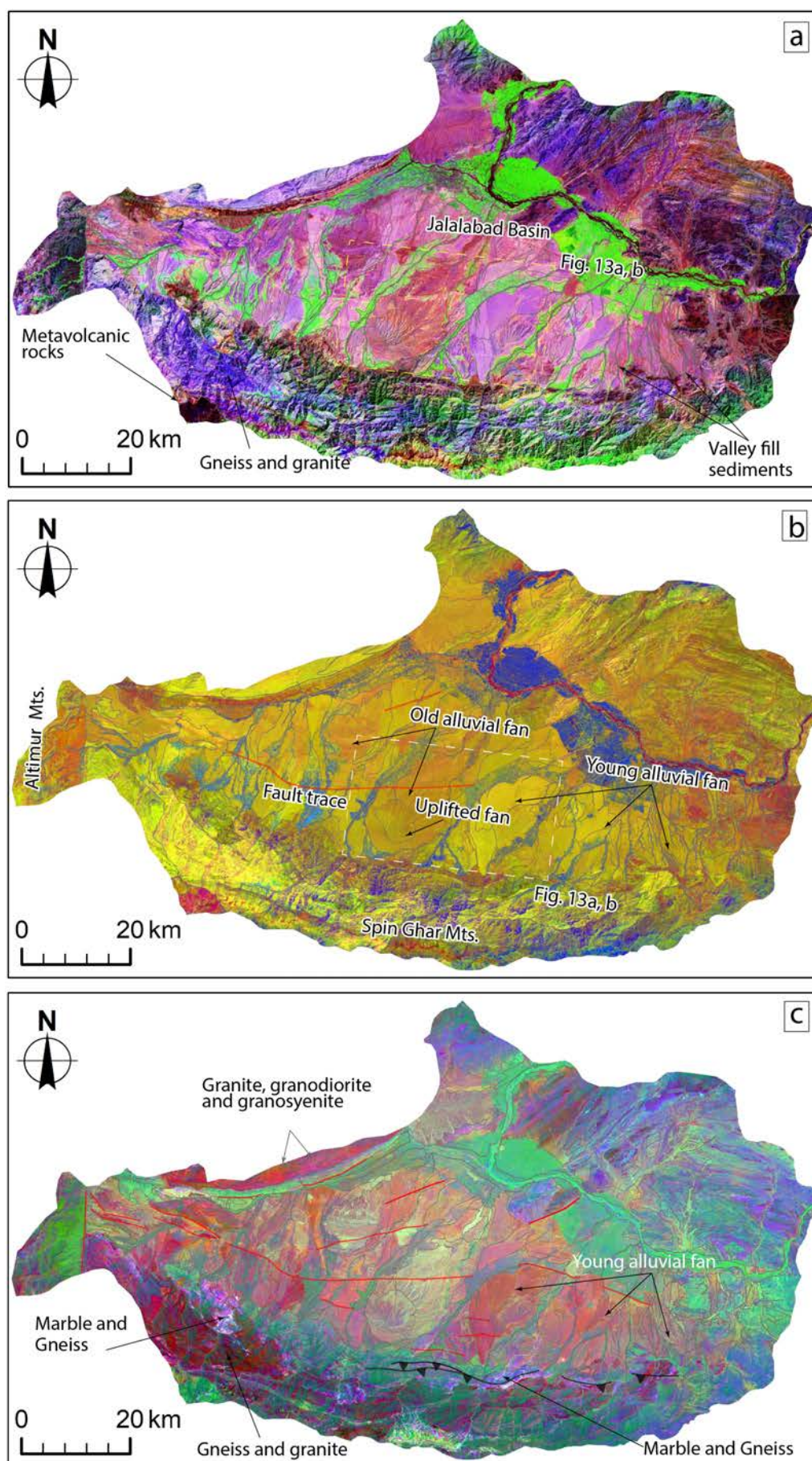


**Figure 4** – Landsat 8 OLI and TIR images displayed as red, green and blue to discriminate lithology of the study area. **a)** Band ratio image 3/2-5/1-7/3, where the dark purple colour shows bedrock contact with the Jalalabad Basin. **b)** Ratio composition of 3/4-7/3-7/6. **c)** Principal component analysis (PCA) image consists of pc 1, pc3 and pc5. The band characteristics are shown in Table 1.

**Table 1** – Characteristics of the Landsat 8 OLI/TIS (Operational Land Imager/Thermal Infrared Sensor) data.

Band No	Subsystem		Spectral Range	Ground resolution (m)	Swath width 185
1	Coastal aerosol		0.433–0.453	30	
2	Blue	Visible (RGB)	0.450–0.515	30	
3	Green		0.525–0.600	30	
4	Red		0.630–0.680	30	
5	Near Infrared (NIR)		0.845–0.885	30	
6	SWIR 1		1.560–1.660	30	
7	SWIR2		2.100–2.300	30	
8	Panchromatic		0.500-0.680	15	
9	Cirrus		1.360-1.390	30	
10	Thermal Infrared (TIRS) 1		10.6-11.19	100	
11	Thermal Infrared (TIRS) 2		11.50-12.51	100	

due to variations in composition. The Jalalabad Basin sediments include alluvial fans, calcrete, flood plain and valley fill sediments (Figure 3a-b). Paleoproterozoic, Palaeozoic, Mesozoic, and Cenozoic bed rock exposures were readily mapped using the Landsat 8 band combination images (Figure 5).

Basement rocks appear in varying shades of maroon to brown in true and false colour band combinations (Figure 3a-b). The Jalalabad metasedimentary rocks north of the Spin Ghar Mountains are distinguished by light pink and violet colours, while the marbles and gneiss are characterized by dark slate-blue colour in the west and south parts of the study area (Figure 3b). The basin is mostly covered by Neogene and Quaternary deposits that constitute a low relief area relative to the bedrock units (Figure 5). Some of the alluvial fan deposits, particularly near to the Spin Ghar Range are older and abandoned, whereas others, mainly along the Kabul River are smaller and actively growing (Figure 3b).

Band ratios (7/5, 6/3, 4/3), (3/2, 5/1, 7/3) and (3/4, 7/3, 7/6) were used to discriminate between bedrock and the various sedimentary rock types (Figures 3c, 4a-b). The (7/5, 6/3, 4/3) band ratios show clear differences between valley fill sediments, alluvial fan and developed calcrete (Figure 3c). In the study area, many of the ephemeral streams have formed their own terraces and deposits. In the (3/2, 5/1, 7/3) bands ratio image, marble and gneiss are distinguished by a medium dark brown, while in the band ratio of (3/4, 7/3, 7/6), the sediments appear as light-dark orange colour (Figure 4a-b). The basin sedimentary rocks distinguish older drier alluvial fans from younger wetter fans based on water content (Figure 4b). The Neogene and Quaternary sediments are characterized by clay content, surface texture and level of dissection (Figure 5). There are different fan types that have been deposited in the area, and the numerous channels show the locations of the coarsest sediments. Dark brown shows the marble and gneiss south of the basin, whereas the dark purple colour displays gneiss and granite along

the Spin Ghar Mountains (Figure 4a). The area highlighted by the dashed yellow rectangle shows particularly good discrimination of sediments by age and sediment type.

The drainage patterns, terraces, old and young alluvial fans can be distinguished easily using PCA. Thus, we were able to differentiate between altered and unaltered rocks in the study area using this method (Figure 4c). The alluvial deposits appear as zones of abundant clay minerals (orange red pixels) in the basin. While the high distribution of sandstone is mostly detected with light yellowish colour (Figure 4c). The schist and gneiss of the Spin Ghar fault block are distinguished from the basin deposits by their light pink-deep pink and deep red colours.

Adjacent to the Spin Ghar Mountains lies the Jalalabad symmetrical basin composed of Neogene (Pliocene) and Quaternary (Early Pleistocene to Holocene) sediments originally deposited on a crystalline basement (Figure 5). Structurally, the Spin Ghar fault movements have caused exhumation incision to the basin deposits, dissection of bedrock terrain, and caused intense folding with east-west and southwest-northeast trends. The unit at the base of the basin sequence is called the Lataband formation and is made up of alternating layers of conglomerates, sandstone and soft clay. Carbonate rocks such as limestone and marl are also present in the area. These formations formed roughly 2 million years ago (Figure 5). The entire sequence of rocks along the fault strands have been gradually deformed into dome-shaped structures by tectonic forces. The rim of this large basin rises a few hundred meters along its southern and western edges.

4.2 Geomorphology and Active Deformation

The study area is structurally enclosed and bordered on four sides by mountain ranges (Figure 2). From south to north, the region can be divided into two main geomorphological zones: the highland folded Spin Ghar Mountain Range and the Jalalabad



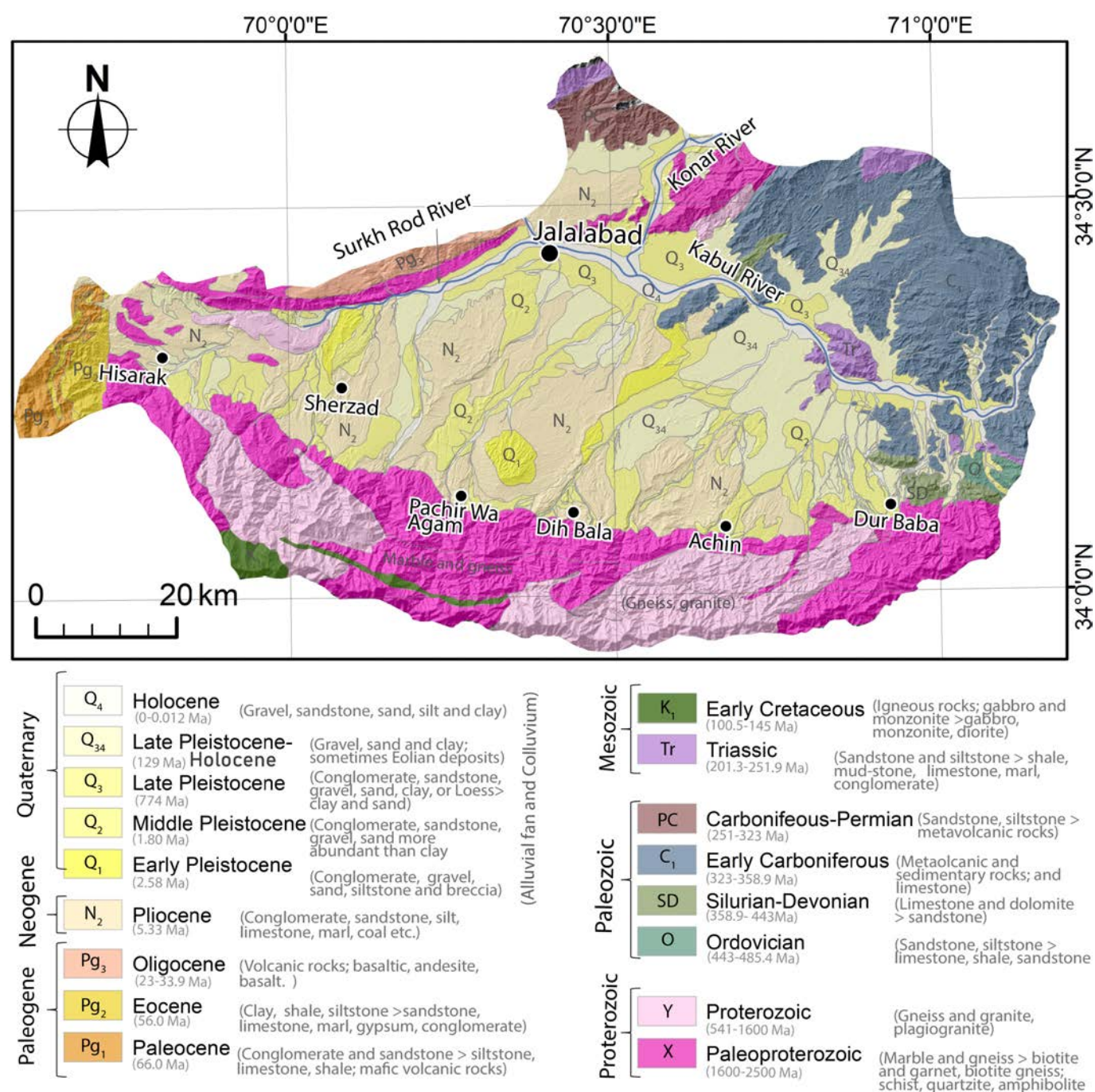


**Figure 5** – Geological map of the Jalalabad Basin from Landsat 8 OLI and TIR data false colour composition, band ratios, principal component analysis and using information from previously published papers. Relative ages of the geological units are modified from Abdullah *et al.* (2008), Abdullah and Chmyriov (1977), Afghanistan Geological Survey (1996), and Doebrich *et al.* (2006). Alluvial fan surfaces of Neogene (Pliocene) and Quaternary (Early Pleistocene to Holocene ages) and bedrock superimposed on SRTM hillshade image. The basin and bedrock terrain are highly dissected by Spin Ghar fault strands.

Basin (Figures 2, 5). The Spin Ghar Mountains Ranges together with the Altimur Mountains form a southward semi-arc that separates the Jalalabad Basin from Parachinar, which is the region from the Indus River west to Paktia Province (Figures 1b, 2). The Spin Ghar Ranges strike east-west and the Altimur Mountain trends mostly north-southeast (Figures 1a, 6). The highest elevation of both ranges reaches 4750 and 4300 m above sea level (asl), respectively (Figure 2). The Spin Ghar Range is characterized by extensively deformed overthrust

anticlines and are composed of marbles, gneiss, granite, gabbro and metavolcanic rocks that are folded and faulted, forming a highly sinuous mountain front (Figures 1, 4).

The Jalalabad Basin is covered by mainly alluvial and colluvial fan debris made of shingly and detrital sediments, gravel, sand, silts, clay and loess ranging in size from fine to coarse grains varieties (e.g., Abdullah *et al.*, 2008; Doebrich *et al.*, 2006) (Figure 5). There are also fine-grained fluvial and lacustrine



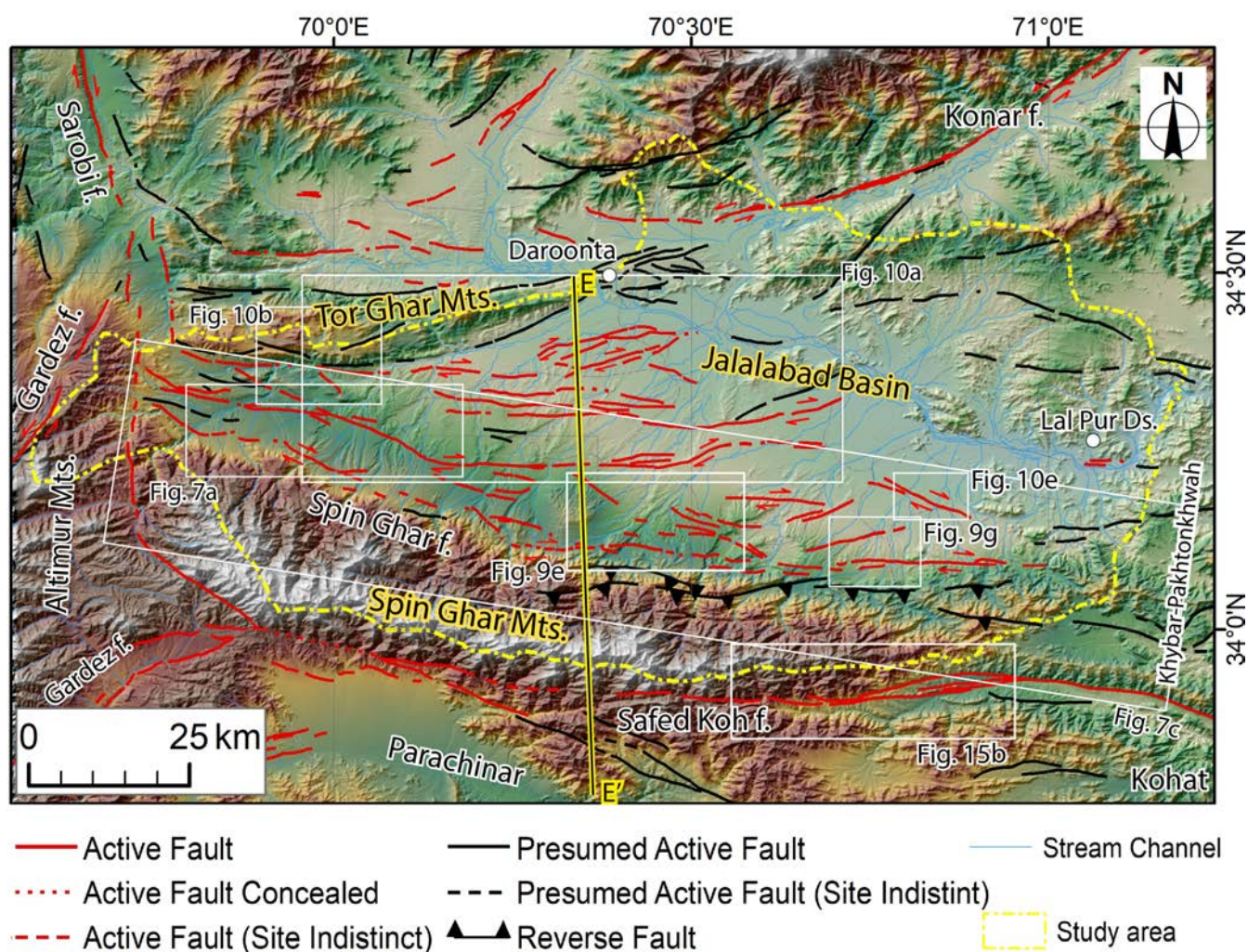


**Figure 6** – Detailed active and presumed active fault map of the Spin Ghar Mountains (Figure 7c) and Jalalabad Basin (Figures 7a-b, 10a). The faults marked by thick red color are the major faults that has evidence of movement in recent geological time. We observed that the major faults cut all materials. Those faults marked by black colour are minor faults that show no clear evidence of recent movement. Active faults are mapped using Landsat 8, three dimensional anaglyph images of 1-arcsecond SRTM, ASTER DEM-30 m, ESRI base map and Google Earth images. Figure 7c displays fault strands associated with mountain fronts, while Figure 10a shows fault strands related to basins; the distinction is based on the tectonic geomorphic features and style of deformation. The line (E-E') refers to geologic cross-section shown in Figure 12.

sediments along both sides of the Kabul River (see Figure 2 for location). This suggests that the Kabul River was at one point ponded, with the re-establishment of throughgoing stream flow causing incision of the alluvial surfaces and the formation of different terraces (Figures 2, 3b). The distribution and degree of dissection of alluvial surfaces suggest that the landforms to the south of the basin are the oldest, which are characterized by very smooth and dark surfaces (Figures 3a-b, 5). The basin deposits range in age from Neogene to Quaternary, overlying the bedrock (Figures 5).

The Jalalabad Basin is wide, with altitude ranging from 500-1800 m asl (Figure 2). The average width of the basin is roughly 45 km and its total length is approximately 120 km. Major antecedent streams emerging from the Spin Ghar Mountains flow across the fault lines to the north-northeast and join the Kabul River (Figures 2, 3c). Topographically, the north-eastern portion of the Jalalabad Basin is

characterized by broad lowlands, including a group of isolated uplands and massifs located between the Daroonta and Lal Pur Districts where the Kabul River passes through this area (Figures 2, 3a). The Kabul River is also a major tributary of the Indus flowing east nearly parallel to the Spin Ghar Mountains, which is characterized by a larger area of drainage in eastern provinces as compared to the north-flowing streams from Spin Ghar Ranges (Figures 1b, 2).

Throughout the basin history it has been deformed internally leading to localised uplift, and subsidence. The prominent evidence of active deformation in the Jalalabad Basin includes uplifted Quaternary-Neogene sediments at an elevation of 500-1700 m, preservation of river terraces of different levels, deflection of stream channels towards the east, and the development of fault scarps offsetting late-Pleistocene and Holocene deposits and landforms (Figures 2, 5, 6).



## 4.3 Active Faults

### 4.3.1 Study Area

The study area is located along the Spin Ghar Mountains close to the Main Frontal Thrust system (Figure 1b). The Spin Ghar Mountains are an east-west trending fold belt that lies in eastern part of the Sulaiman fold thrust belt and western part of the Kohistan Arc (Figure 1a-b). The ridge also separates the Parachinar quadrangle from eastern Afghanistan and the bedrock terrain from the Neogene-Quaternary alluvial filled basin (Figures 1b, 5). The Quaternary deformation in the region is mostly driven by north and northwest-ward contraction between the Indian and Eurasian plates (Figures 1a, 5). The regional and local tectonic activities form a basin and range type horst and graben topography (Figure 2). Most faults that we identified in the folded region are southeast-dipping thrust faults with sets of arcuate fault scarps (Figure 6). Many prominent geomorphic features such as fault scarps, offset surfaces, tilted alluvial fans, folds and pressure ridges were observed along the active fault traces (Figures 6, 7a-b). Strike-slip movement as inferred along some faults from lateral stream displacement and offset quaternary terraces (Figure 6).

The broad-scale deformation in the area can be explained by southeast-dipping thrust and strike-slip faults interacting with major rivers and minor tributaries (Figure 6). The major active Spin Ghar fault consists of multiple fault strands representing different segments of the larger fault system. To better understand the active deformation along the Jalalabad Basin, we mapped the Spin Ghar fault in detail (Figure 6).

### 4.3.2 Spin Ghar Fault

The Spin Ghar fault system is one of the major active faults in eastern Afghanistan, extending ~130 km in an east-west direction, with oblique thrust and right-lateral slip (Figure 6). The fault starts from the eastern frontier of the Kabul Block and stretches continuously from its junction with the Sarobi right-lateral strike-slip fault to the border region with Khyber-Pakhtunkhwa (Figure 2). The Spin Ghar fault trace is sinuous, and extends parallel to the Spin Ghar Mountain Ranges (Figure 6). This fault separates the Spin Ghar Block from the Konar Block located to the north (Figure 1b). Generally, the fault consists of multiple fault strands along the Jalalabad Basin. Although some strands of the fault are concealed under the recent deposits, overall it is clearly expressed in the geomorphology and identifiable in high-resolution satellite images (Figure 5, 7a-b).

The general relief of the study area contains mountainous uplifts and depressions (Figure 6). The southern side of the Spin Ghar fault is uplifted while the northern side is depressed (Figure 2).

The Spin Ghar fault splays into several synthetic strands mostly in the Jalalabad Basin (Figure 3a). The east-west striking fault strands are densely distributed in the western part of the basin in Hisarak District (Figure 7c). They have displaced young geomorphic surfaces resulting in the development of prominent south-facing fault scarps inside the basin (Figures 6, 7a-b). The fault strands are largely concentrated within the tectonic bulge within the basin interior. Several discontinuous southwest-facing thrust fault scarps are mapped along the northern front of the Spin Ghar Mountain Range (Figure 6). The uplifted area is closer to the fault scarps that are highly incised and eroded with deflected and beheaded channels (Figure 2). These scarps are characterized by topographic breaks, warped alluvial deposits and tilted fans. The fault scarps are lower in the eastern side of the Jalalabad Basin and higher in the west in Hisarak, Sherzad and Khogyani Districts as the relief of the drainage basin is reduced towards the north (Figure 7a-c). The height of the scarps is different from place to place, which ranges from <1 m to 90 m along the basin (Figure 8a). In the northeastern side of the Jalalabad Basin, the scarp heights are reduced and eventually disappear toward the Kabul River flowing from the west to the east (Figures 7a, 2). We divided the Spin Ghar fault system into two sections based on the tectonic geomorphic features and styles of deformation observed along each (Figures 6, 7c).

#### a) Mountain front fault strands

The southern section of the Spin Ghar fault extends along the northern foot of the Spin Ghar Mountains from Hisarak District to Dur Baba (Figure 7c). Several shorter fault traces are also observed along the mountain front, which cut recent and older alluvial fan (Figures 7c, 9a-c). Here, the Spin Ghar fault scarp is south-facing and also shows right-lateral stream offsets (Figure 7b-c). In Sherzad District, an alluvial fan surface shows the largest identified right-lateral offset of  $\sim 600 \pm 70$  m in the area (Figure 9a-b). In Pachir Wa Agam District the fault strand cuts an alluvial fan surface of Late Pleistocene or Late Pleistocene-Holocene age (e.g., *Abdullah and Chmyriov, 1977; Doebrich et al., 2006*) (Figures 5, 9d-f). The fault scarp in these alluvial fans varies in height from 1 m to 20 m (Figure 8b). Near to this offset surface we also mapped thick uplifted and incised fans, which show movement along some fault strands ( $34^{\circ}9'55.01''\text{N}$ ,  $70^{\circ}20'18.54''\text{E}$ ) (Figure 9e).

From Sherzad to Parchir Wa Agam Districts, we identify a restraining double bend associated with an uplifted terrain and a south-facing scarp (Figures 7c, 9d). The area from Parchir Wa Agam District to Dur Baba has two fault strands that are right-lateral oblique thrust faults extending into the bedrock (Figure 7c). The first fault strand (marked with number 1) in southern part of the basin has no clear lateral offset, but the geomorphic expression is clear along most of its trace. The total length of this strand



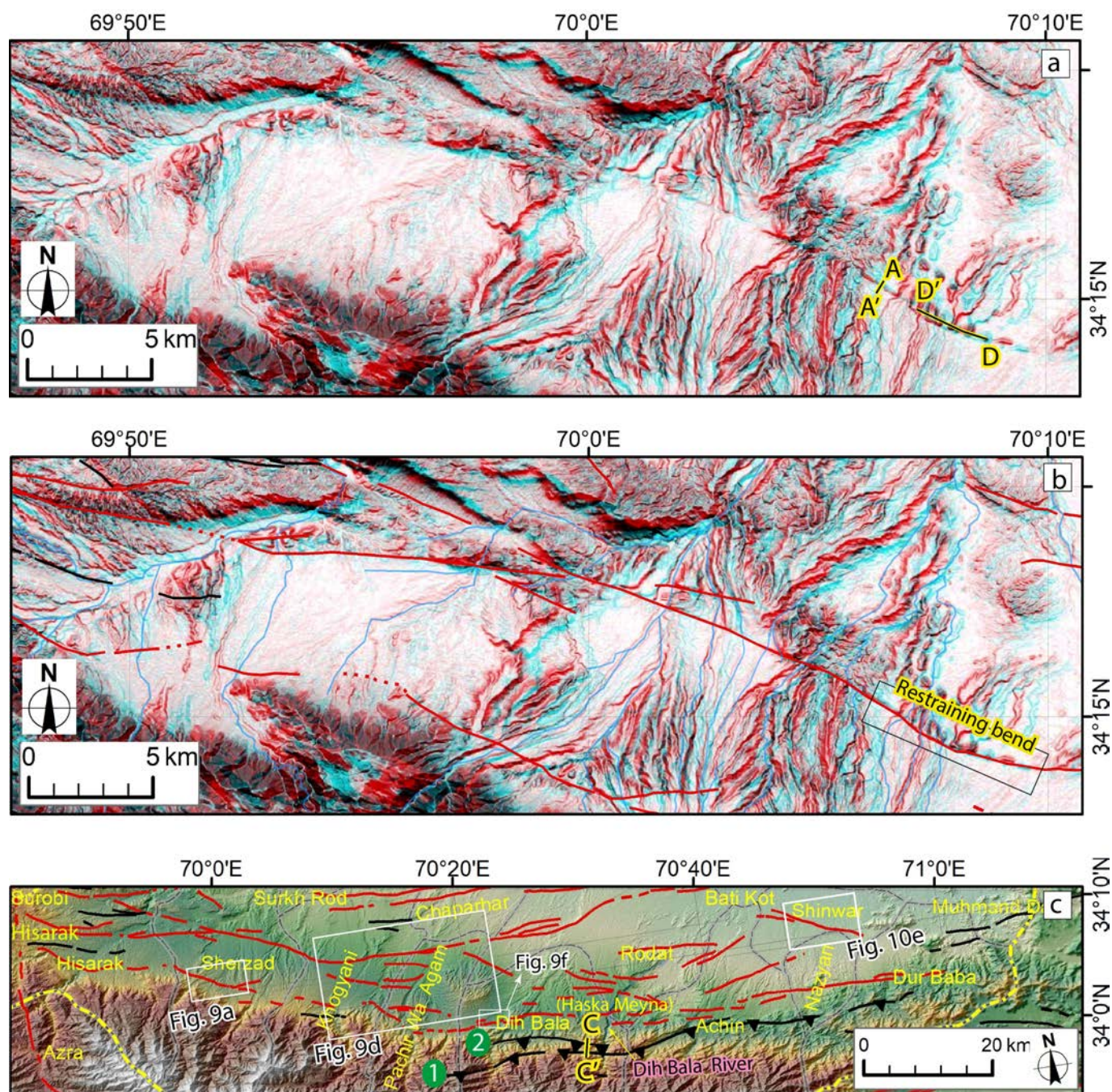


**Figure 7** – **a)** Anaglyph image of the western segment of the Spin Ghar fault system. The geomorphic expression of the fault in Quaternary and Neogene landforms and deposits varies along the fault trace. The fault movement offsets older and younger alluvial fans, stream deposits and channels (as shown in Figure 5). The lines (A-A') and (D-D') refer to the topographic cross-section shown in Figure 8a, d. **b)** Anaglyph image is overlain by the active fault strands distribution and uplifted area. A bend structure associated with an uplifted terrain making a south-facing scarp is also shown in the figure. **c)** Place names and detailed map of the Spin Ghar fault along the Spin Ghar Mountain front. Legend is the same as shown in Figure 5. The referenced lines (B-B') and (C-C') indicate topographic cross-section shown in Figure 8b-c.

is more than 65 km. Another segment of the thrust fault in bedrock is marked with number 2 (Figure 7c). This fault is north of the first strand, and extends for 12 km further east. The northern strand of this segment is associated with a south-facing cliff-like scarp (Figure 8c). This fault follows a linear valley of the Haska Meyna or Dih Bala River (Figures 3b-c, 7c). Further east, the fault is obscured under bedrock terrain, but within the valley the bedrock ridges mark the location of the fault trace. In the border region

with Dur Baba District, we mapped the fault strands as presumed active faults because the fault trace is expressed as a topographic lineament (Figures 6, 7c). This segment extends for >15 km in the east-west direction, and is characterized by a linear valley.

In some places, alluvial fans and bedrock are separated by the fault (Figures 5, 9d), from which we infer thrust faulting along with a component of right-lateral strike-slip. A 1.5 km line of pressure



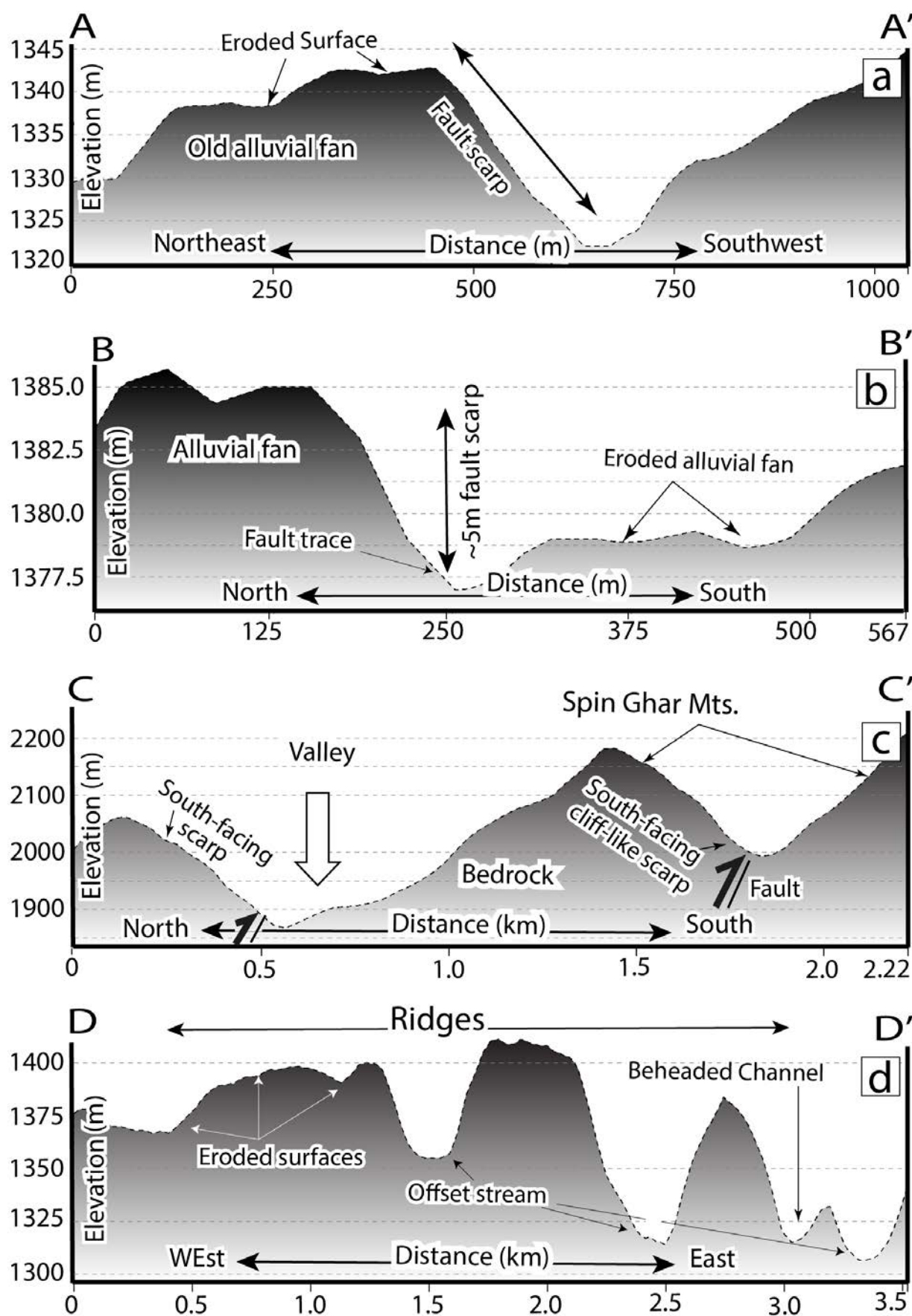


**Figure 8 – a)** Profile across the Spin Ghar fault trace in Sherzad District. **b)** A topographic profile across a fault strand in a young alluvial fan. In this place, the fault scarp is around 5 meters high. **c)** Profile along the two thrust faults along the northern front of the Spin Ghar Mountain that shows south-facing scarps. **d)** Longitudinal profiles along ridges showing southern-facing scarp, and are cut by ephemeral streams flowing from south (Spin Ghar Ridges) to north (Jalalabad Basin). The location of the profiles are shown in Figures 7a and 7c.



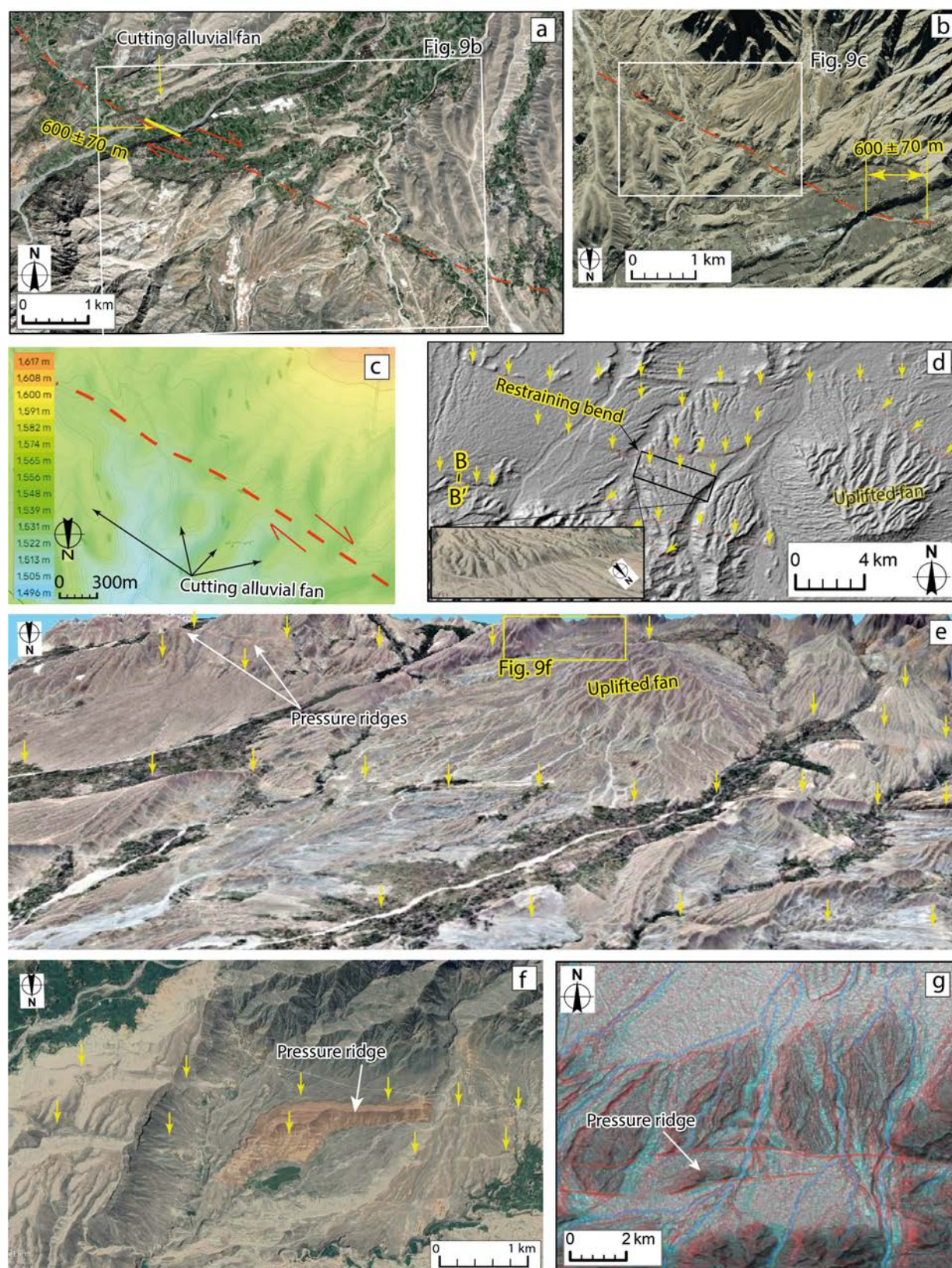


**Figure 9** – **a)** ESRI base map of the Spin Ghar fault offsetting alluvial fan and stream deposits along the range front. Red dashed lines show surface fault traces. The image location is shown in Figure 7a. **b)** Larger 3D view of the same alluvial surface as shown in Figure 9a. The maximum stream offset is about  $600 \pm 70$  m. **c)** Topographic map of the alluvial fan shown in Figure 9b. **d)** The Spin Ghar fault cuts through the range front alluvial surface. Yellow arrows mark active fault traces. **e)** Perspective 3D view of typical alluvial fan located in Jalalabad Basin. **f)** Google earth image of the offset alluvial fan shown in Figure 9e. **g)** The strike-slip Spin Ghar fault. The fault trace is convex to the south and has both continuous and discontinuous sections of arcuate scarp developed in range front alluvium and cross-cutting Spin Ghar bedrock terrain.



ridges along the adjacent alluvial fan indicate fault activity during middle Pleistocene (e.g., *Abdullah and Chmyriov, 1977; Doebrich et al., 2006*) (Figures 5, 9e-f). The pressure ridges trend east-west and are cut by the north-flowing river (Figures 2, 6). The middle and late Pleistocene deposits along the mountain front consist of conglomerates, sandstone and clay. These formations are extremely dissected by the Spin Ghar fault strands (Figures 5, 9g).

### b) Basin fault strands

Several fault strands traverse the Jalalabad Basin interior (Figures 6, 7a-b, 10a). We identified active fault scarps and surface deformation both along the Tor Ghar Mountain front and Jalalabad Basin (Figures 2, 10a-b). Most of the fault strands are east-northeast-striking right-lateral oblique thrust type. Major cross cutting oblique thrust faults are located in the central and southwestern portion of the basin. The timing of the shortening is constrained by the Pliocene to Late Pleistocene-Holocene deposits (Figures 1a, 5).

The Tor Ghar Mountains form the western boundary of the Jalalabad Basin (Figure 10a). The fault along the Tor Ghar Mountain front is concave to the east (Figures 6, 10a-b), and separates alluvial fans from bedrock. The fault strands along the mountain front are expressed in alluvial fan deposits and are east- and slightly northeast-trending (Figure 10b). We also observe pressure ridges formed adjacent to the fault in the alluvial fans (Figure 10c). From west to northeast, the fault traverses the broad valley along the Khogyani and Surkh Rod Districts (Figure 10a). To the north, the fault zone splays into multiple strands in the Tor Ghar bedrock terrain (Figure 10b). These fault strands appear to merge with the northern Konar fault system, which is an active left-lateral strike-slip fault (Figure 1a, 6).

The fault trace marked with number 3 consists of several stepping fault traces extending for several kilometres within the basin (Figure 10a) and traversing small uplifts (Figures 7a-b, 10d). At the eastern edge of the Jalalabad Basin, one can see the fault trace on a young alluvial fan (Late Pleistocene-Holocene), showing ongoing activity on the fault (Figures 5, 10e). Some of the topographic features mapped in this area are similar to the fault segments along the Spin Ghar Mountain front (Figures 6, 7c). Continuous oblique right-lateral stream offsets illustrate the central part of the fault (Figures 7a-b, 10a). The fault scarp extends for over 70 km and separates the elevated southern part from the northern downthrown area. The scarps seem highly eroded with offset and beheaded channels (Figure 10e). Along the fault, pressure ridges have formed on the alluvial fans that emerge from the adjacent surface, indicating that the ridges have been uplifted after being deposited by rivers flowing from south to north (Figures 7b, 8d). In the Khogyani District (34°13'55.39"N, 70°15'28.26"E), a ridge deflects the river right-laterally (Figure 6).

The ridges are mostly composed of conglomerates, sandstone, shingly and detrital sediments (Figure 5). Due to vertical motion along the fault, the southern edge of the basin is being uplifted (Figures 6, 7a-b, 9e).

Another splay fault marked by number 4 in Figure 10a is interpreted along the Jalalabad Basin along the northern side of the Spin Ghar Mountains. This fault strand is an east-trending right-lateral strike-slip fault. The faults have right-laterally displaced alluvial fans by tens to hundreds of meters (Figure 10f-g). The geomorphic expression becomes less clear further east toward the Bati Kot District (Figure 10a). We measured the fault scarp height at ~50 m using the 1-arcsecond SRTM DEM (e.g., Figures 8a and 10f-g). This fault segment traverses for more than 40 km approximately parallel to the ridges that were mapped along the fault strands marked with number 3 (Figure 10a).

In the eastern part of the Jalalabad Basin, we mapped a presumed or potentially active fault marked by number 5 that extends northeast for 15 km from the start of the Rodat District to the Kabul River (Figure 10a). The fault scarps merge with the fault marked by number 4 in Rodat District. The geometry of this fault is poorly known because the fault mostly traverses low-lying bedrock terrain with thick alluvial deposits and stream channel offsets (Figure 10a). We consider that the fault crosses the mountainous area along the north-eastern ridge.

The number 6 splay fault strand is >20 km in length. This fault is also parallel to the fault marked by number 4 (Figures 6, 10a). Along the fault, we identified scarps no more than a few meters high on alluvial lowlands (Figure 11a). This represents freshly broken, back-tilted and warped depositional surfaces. The deformation is attributed to long-term displacement on the fault. The fault is mostly in Neogene (Pliocene) deposits, but to the northeast the fault also has a visible trace in Late Pleistocene deposits (Figures 5, 6).

A series of oblique strike-slip fault strands also define the northern boundary of the basin, which form linear scarps in Middle-Late Pleistocene to Holocene formations (Figures 5, 6, 11b). The northern margin of the basin is dominated by low land approximately 530 m above sea level in vicinity of the Jalalabad City, which is cut by southwest-northeast striking faults (Figures 2, 6). The fault lines are located 4 km east of Tor Ghar Mountain and are marked by number 7 on Figure 10a. These fault lines run parallel to the steep slope of Tor Ghar Mountains (Figure 11b). A gentle convex slope to the north extends farther to the Kabul River (Figures 2, 10a). We identified several small scarps that trend north-northeast. Some of the scarps face northwards along the basin close to the Kabul River (Figures 10a, 11c-e). The small scarps extend along the flat depositional surfaces throughout the basin (Figures 5, 6). Thus, it is assumed that these scarps are formed through



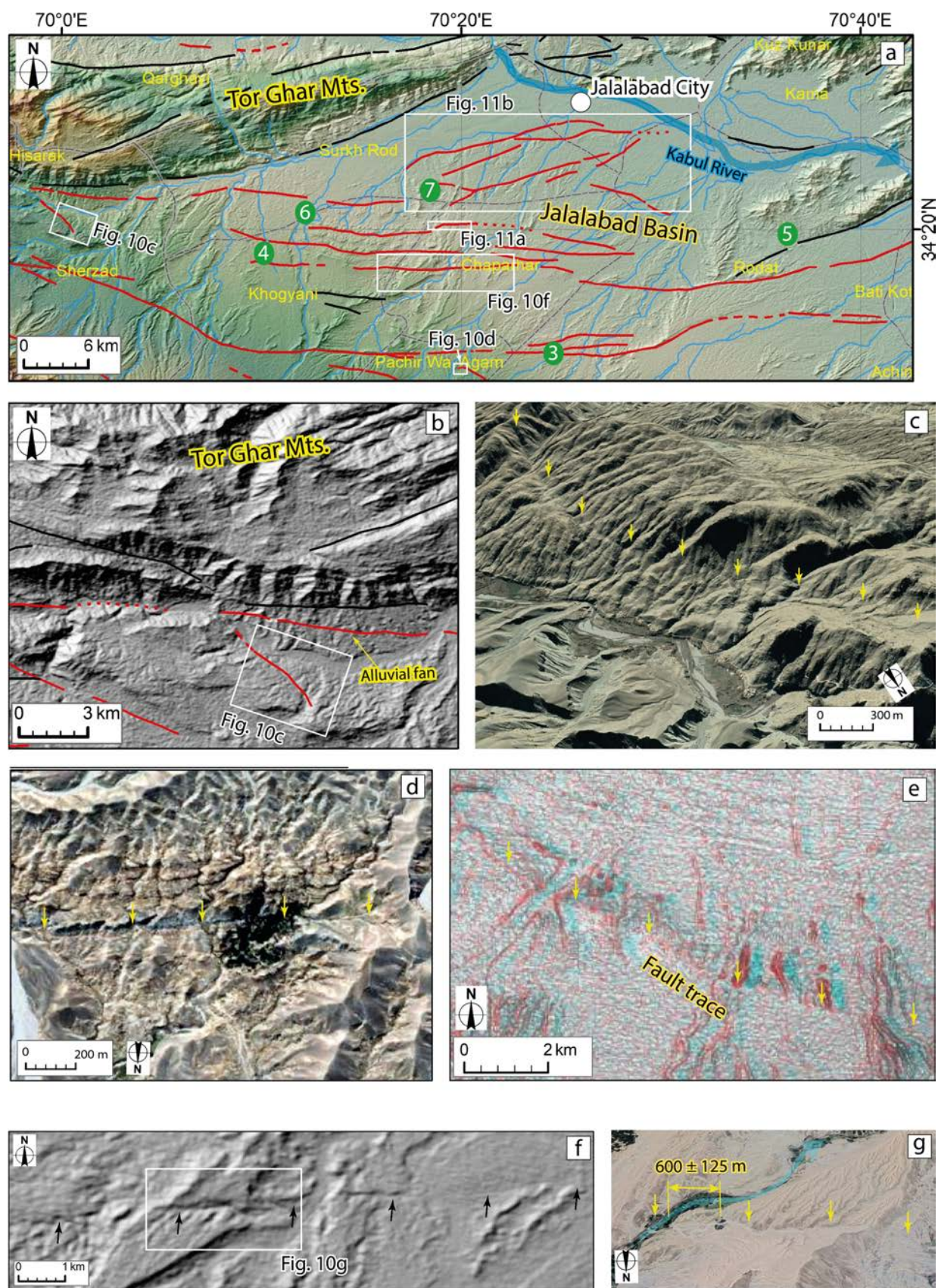


**Figure 10** – **a)** Spin Ghar fault system on northern side of the Jalalabad Basin. The numbers in circles show various fault strands in the basin. **b)** Spin Ghar fault strands along the Tor Ghar Mountain. **c)** 3D map view of the fault strand offsetting Quaternary deposits in the Jalalabad Basin. **d)** Offset surfaces developed in Neogene rocks along the northern side of the fault. **e)** This image combines anaglyph and hillshade techniques to show the contact fault trace in the young alluvial fans located in eastern part of the Jalalabad Basin. **f)** Hillshade map of features associated with active tectonics. The black arrows locate active fault traces that offset different age surfaces. **g)** ESRI base map image of the same fault strand that is shown on Figure 10f. The yellow arrows shows the surface fault location.



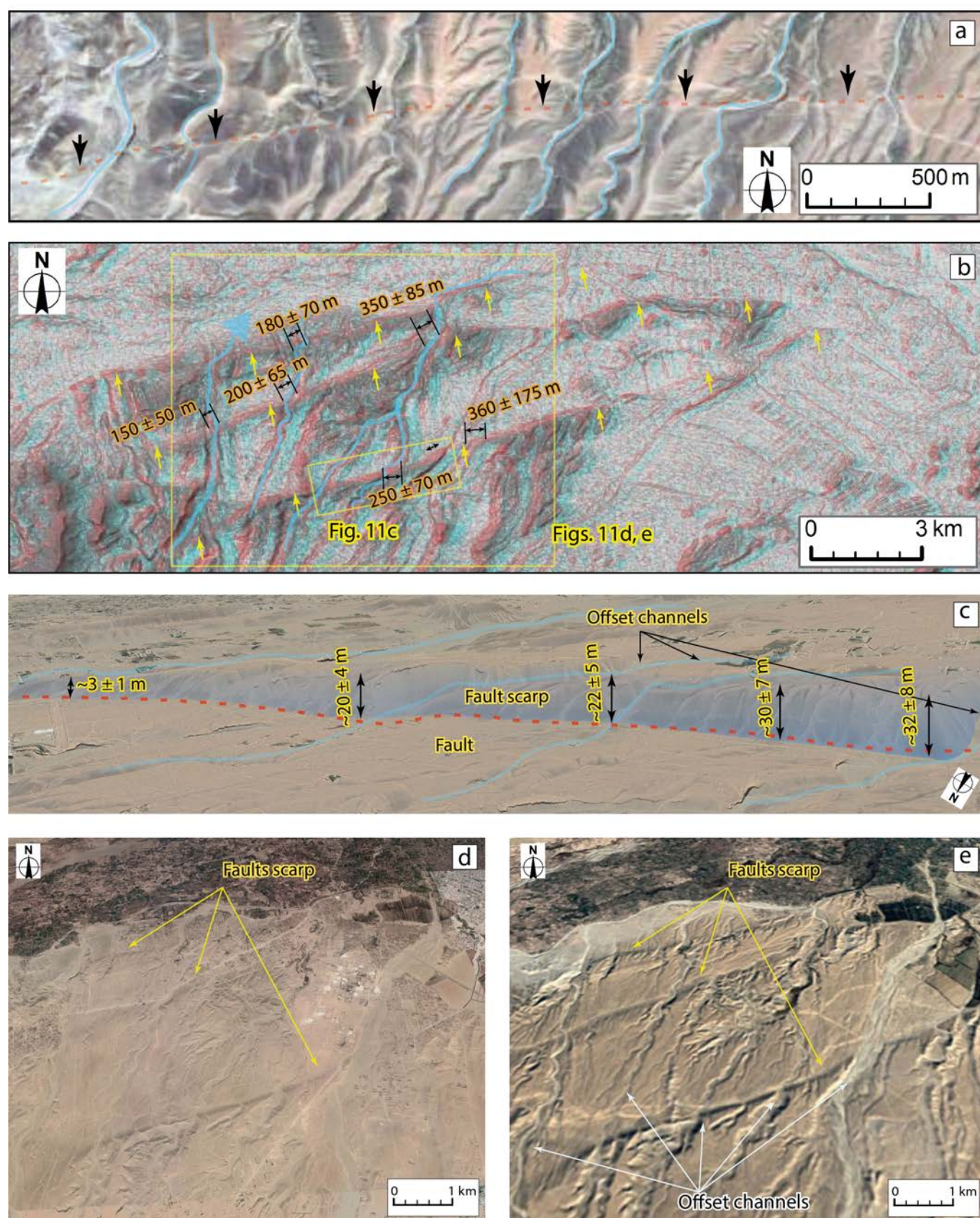


**Figure 11** – **a)** ESRI (Environmental Systems Research Institute) basemap image of offset ephemeral stream channels and a fault strand of the Spin Ghar fault. **b)** Northeast-trending strands of the Spin Ghar fault near to Jalalabad city showing evidence of oblique thrusting as indicated by black arrows. The fault offsets Late-Pleistocene surfaces. **c)** Google Earth 3D view of the offset alluvial fans and ephemeral stream channels that have been displaced both right-laterally and vertically by strands of the Spin Ghar fault. **d)** Google Earth image of the same area with imagery date 2017. **e)** Google Earth image of the same area captured in 1985. Since 1985, the fault scarps have degraded due to landscape alternations by farming and building constructions.



recent faulting events in the study area. The study area has a semi-arid climate, which means that there is also a possibility that the fault scarps could be quite old without significant modification. To verify one of these assumptions, it's important to use a combination of methods, including field observation and dating techniques.

The main river shows a marked offset in Surkh Rod District (Figures 10a, 11b-c), with deflection to the northeast right-laterally before meeting with the Kabul River. The faults near the southwest margin have prominent scarps whereas the scarps fade toward Jalalabad City and northeast near to the Kabul River (Figures 2, 10a). Recent deposition or erosion by drainage and human activities has been suggested to have destroyed several fault scarps (Figure 11b-e). The quaternary faulting resulted in significant tilting of the Pleistocene alluvial deposits (Figures 5, 6). The prominent fault scarps show that they have been formed by oblique thrust faulting as a result of ongoing active deformation in the region (Figures 10a, 11b).

## 5 Discussion

The deformed basement of the Jalalabad Basin consists of Proterozoic metamorphic rocks, exposed in the drainage area of the Spin Ghar fault system (e.g., *Abdullah et al., 2008*) (Figure 5). South of the basin, the Spin Ghar Ranges have been deformed by strike-slip and reverse faults (e.g., *Ruleman et al., 2007; Shnizai, 2020a*) (Figures 6, 12). The Spin Ghar Block is underlain by 4500-8000 m thickness of strongly metamorphosed Proterozoic rocks, which are intruded by subconcordant bodies of Proterozoic granites (*Abdullah et al., 2008*) (Figures 1b, 5). According to *Denikaev et al. (1971)*, cited in (*Abdullah et al., 2008*), the metamorphic rocks of this block form three units: lower, middle, and upper (Figure 5). The lower unit consists of gneiss, quartzite, and schists, which outcrop in the cores of anticlines in the watershed portion of the ridge. The middle unit consists of thick light grey and white marble layers alternating with biotite gneiss, garnet-biotite schist, quartzite, and amphibolite, which outcrop along the northern slope of the block. The upper unit is a monotonous sequence of dark-grey and silvery-grey biotite, garnet-biotite, muscovite-biotite, garnet, and other schists including marble interbeds. This unit of metamorphic rocks is exposed in small outcrops along the northern foothills of the ridge. *Abdullah et al. (2008)* stated that small gabbro-diorite bodies of supposedly early Cretaceous age occur in the western part of the block. The formation of Lower Carboniferous age is widespread at the southern foothills of the ridge. The Jalalabad Basin is filled with continental fine to coarse-terrigenous deposits that have grey and red to variegated colour (Figure 3a-b). These deposits belong to the Neogene and Quaternary (Figure 5). The Neogene deposits are overlain unconformably by Quaternary units.

Tectonic activities in the region have influenced the alluvial fans in the basin. The alluvial fans are coarse and thick, and are deformed showing the area is tectonically active (e.g., *Leleu et al., 2009*) (Figure 12). In Figure 13a-b we suggested restoration of Pliocene rocks and alluvial fans from Landsat 8 multispectral data (band ratio of 3/4, 7/3 and 7/6), showing that the Spin Ghar Fault system has a total horizontal offset of less  $900 \pm 140$  m. The offset geomorphic surfaces and ephemeral stream channels have been interpreted to result from Late Quaternary (Holocene and Late-Pleistocene) cumulative offset (Figure 5).

The active tectonics of eastern Afghanistan appears to be dominated by the northeasterly trending left-lateral Chaman, Gardez, Paghman, and Konar faults, and the east-west Spin Ghar, Safed Koh and Sarobi oblique right-lateral faults (Figures 1b, 14, 15a). The surface expression of the Spin Ghar active fault trace within the Jalalabad Basin is discontinuous and segmented (Figures 2, 6), though we assume these traces are part of a more continuous zone at depth (Figure 12). Across the Jalalabad Basin, we have created a schematic cross-section that includes a topographic profile, geological units, faults, and structures based on our mapping (Figure 12). We assumed the geometry of the faults at depth based on the fault strike, the presence of offset geomorphic features, and seismicity (Figures 5, 6, 15a). The Spin Ghar fault system is made up of a series of parallel reverse and right-lateral fault strands. In the basin, we have also observed several anticlinal structures that have an east-west direction. The structures are deformed in a step-like pattern, and which rotate clockwise about a vertical axis to accommodate the overall north-south left-lateral tectonic plate movement. Therefore, the Spin Ghar oblique fault strands appears to be part of a zone of bookshelf faulting where regional left-lateral faulting is accommodated at northern end of the main thoroughgoing Chaman left-lateral fault (Figure 12). The evidence for quaternary activity along the west-trending, south-stepping Main Boundary fault systems and Safed Koh fault indicates that the Main Boundary fault consists of an active duplex thrust system with multiple south-verging imbricate thrust faults (*Ruleman et al., 2007*) (Figure 1a-b).

According to *Tapponnier et al. (1981)*, eastern Afghanistan and the Sulaiman-Kirthar Mountain Range structures may have formed by inverting earlier continental margin structures, and the deformation associated with India-Afghanistan convergence during Plio-Pleistocene times shows increasingly transpressive features (Figure 1a). Furthermore, the appearance of the mountain-front morphology, shutter ridges, and south-facing fault scarps all point towards an increasing component of reverse faulting (Figure 1). According to *Mcdougall and Hu (1991)*, the sequence of thrust faults accounts for 50% shortening in Tertiary sediments. In this area, blind thrust faults have twice the amount of horizontal shortening compared to the faults that



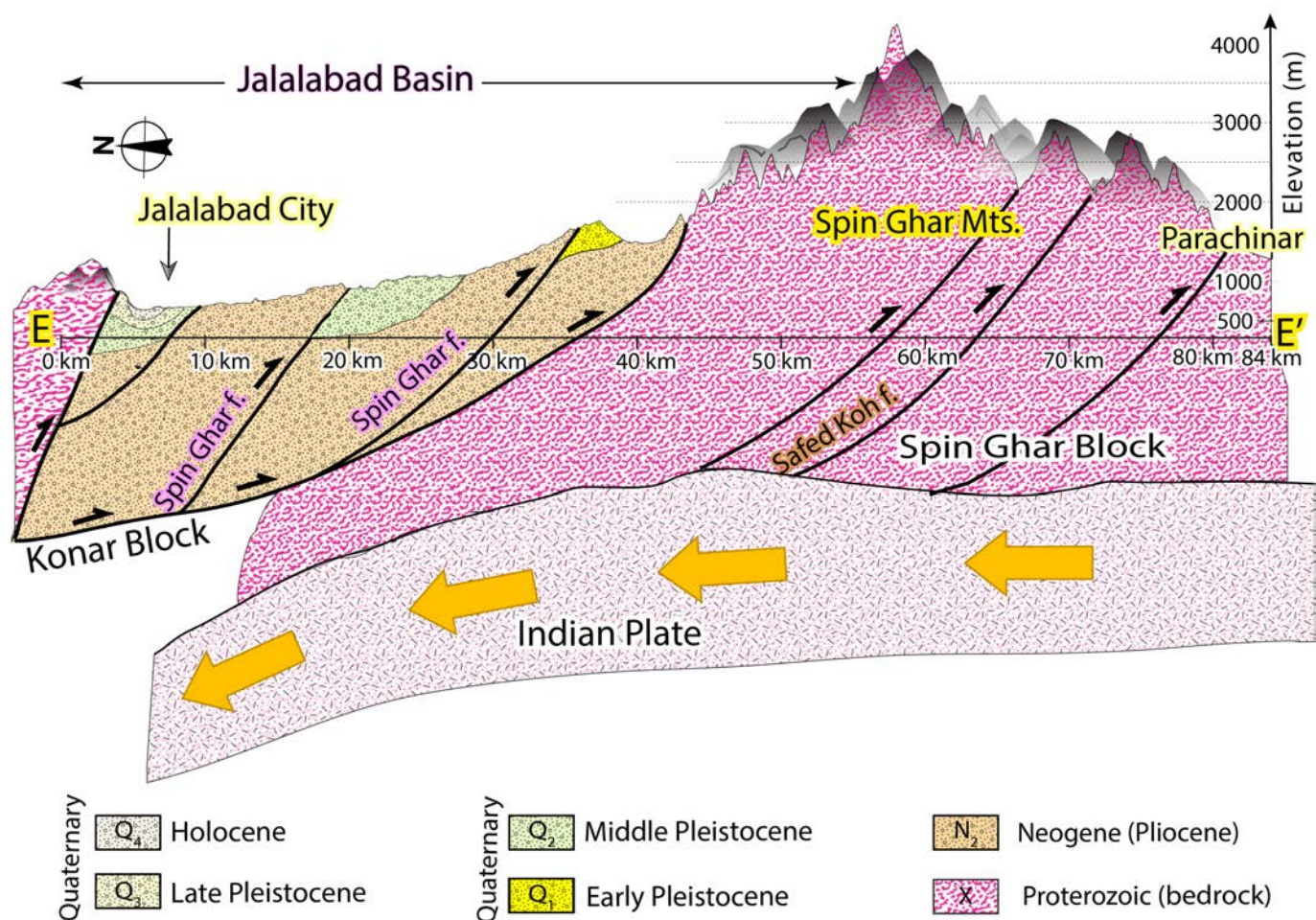


**Figure 12** – Schematic geologic cross-section across the Jalalabad Basin showing how strands of the Spin Ghar fault are lined to merge onto a decollement beneath the Jalalabad Basin, and connect to deeper structures in the north. The Spin Ghar reverse and right-lateral faults are likely part of a zone of bookshelf faults, accommodate continues north-south left-lateral shear across the region.

are mapped on the surface. The blind structures may be responsible for some of the hidden seismicity in the folded region.

The Main Boundary Thrust and its surrounding areas are home to numerous active faults, which primarily exhibit east-west trending dips (Figure 1a). These kind of faults mostly developed in the western part of the Parachinar as well as close to, or on, the Main Boundary Thrust (e.g., *Nakata et al., 1991*) (Figures 1b, 12, 14). *Nakata et al. (1991)* reported that in many places Quaternary gravel on the eastern front of the Sulaiman Range shows considerable tilting toward the east (Figures 1a, 15a). They also stated that the Middle Pleistocene age alluvial fans are offset vertically by ~20 m. This suggests that the Safed Koh faults are present along the full length of the Parachinar to Kala Chitta fold belt south of Peshawar (Figure 1a). The Safed Koh fault has both continuous and discontinuous Quaternary expression along sections of the range front and proximal piedmont deposits extending from the Parachinar Region to north of Salt Range close to Peshawar (Figures 1a, 15b). In particular, the northern section of the fault is

characterized by discontinuous scarps in bedrock terrain. The preservation of bedrock scarps in this terrain suggests recent activity during the late Quaternary (Figure 1b).

North-northeast of Peshawar, north-south trending active faults and active anticlinal axes can be found along the southwestern part of the Spin Ghar Mountains (Figures 1a, 2). In this area, a series of possibly active faults are recognised. Generally, active dip-slip faults with various strikes are widely distributed in the region. The Safed Koh fault together with other faults define a network of south-verging thrust faults (e.g., *Ruleman et al., 2007*) (Figures 6, 15b). The present deformation is considered as the continuation of Late Paleogene crustal shortening that developed in response to the collision between Indian and Eurasian plates (Figure 1a). The quaternary deformation seems to be partitioned between conjugate shear zones and south-verging thrust faults, which indicates that there is a complex interplay between faults in this region (Figures 1a, 14, 15a).

On Figures 14 and 15a we show the mapped active faults, along with earthquake occurrences,



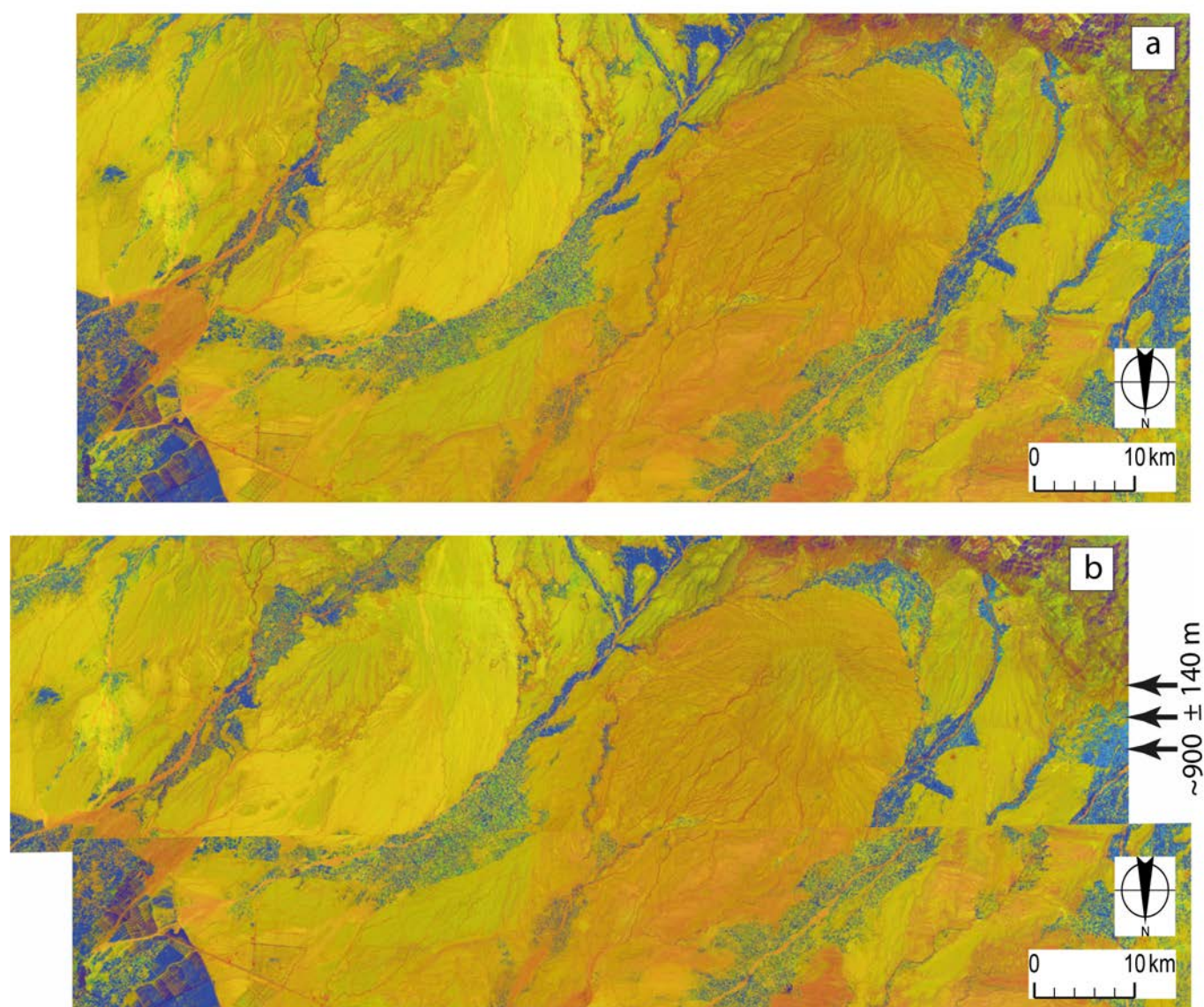


**Figure 13** – Restoration of displaced alluvial fan in the Jalalabad Basin. **a)** Landsat-8 OLI/TIS bands ratio (3/4-7/3-7/6) image. **b)** The slip restoration of the Neogene-Quaternary (middle-early Pleistocene) alluvial fan in the basin. The alluvial fan is restored by  $\sim 900 \pm 140$  m to its pre-faulting position. The image location is shown in Figure 4b.

including those reported in historical records (red circles with magnitude  $\geq 6.0$ ), and those determined from instrumental data (yellow, green and blue circles) (e.g., Dewey, 2006; Ekström *et al.*, 2012; ISC-EHB, 2023; USGS, 2023). Although there is relatively large uncertainty on the locations of historical major earthquakes, large earthquakes and surface faulting have occurred on some of the mapped active faults observed in the satellite images (Figures 6, 15a). The Global Centroid Moment Tensor (CMT) Catalogue suggest that the east-west-striking thrust faults are active and can be valuable in producing seismicity (blue circles). Estimated depths in the Global CMT Catalogue and USGS shows that the earthquakes striking east-west occurred at depths of  $\geq 10$  km (Figure 15a). In the western part of the study area the earthquakes have strike-slip faulting mechanisms, but inside the Jalalabad Basin and Spin Ghar Block the earthquakes have reverse and oblique faulting (Figure 6). These reverse and oblique slip faults within

the basin and more widely in eastern Afghanistan may have been important in accommodating some of the relative motion between the Indian and Eurasian plates (Figures 1a, 14, 15a). Dewey (2006) reported that the shallow-focus earthquakes (green circles) across most of eastern Afghanistan reflect the northward movement of the Indian earth's crust and mantle with respect to Eurasian plate (Figure 1a). Most of these faults are often major source for seismic hazard, but there are no clear geomorphologic observations along the fault traces to confirm their activity. Shallow activity seems to be associated with the Sarobi, Konar and Spin Ghar faults (e.g., Prevot *et al.*, 1980) (Figures 1a-b, 14).

Although the total displacement on the above faults is large, the rate of active slip is unknown, and must be calculated from the division of the accumulated offset (alluvial fan, gullies, etc.), by any absolute age dating of the corresponding geological



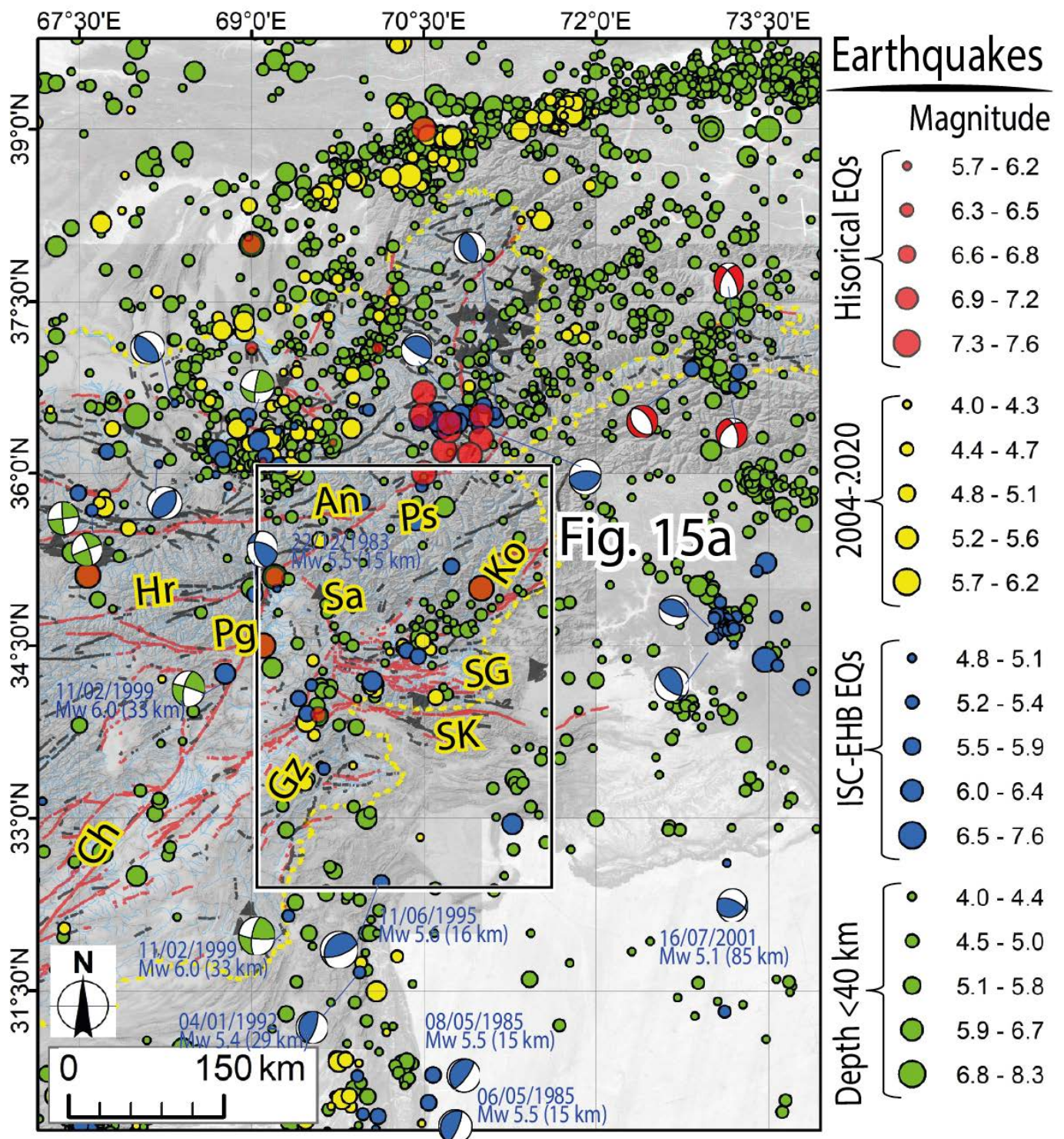


**Figure 14** – Seismicity map of north-eastern Afghanistan. The map was constructed using earthquake catalogue prepared by Dewey (2006), which includes crustal seismicity at depths less than 40 km with  $M \geq 4.0$  recorded from 1900-2004. Red circles are locations of documented historical earthquakes. Yellow circles show location of earthquakes from 2004-2017 recorded by International Seismological Centre (ISC-EHB, 2023). The blue circles show locations of earthquakes with magnitude  $\geq 5$  recorded by Global CMT catalog (Ekström *et al.*, 2012). The green circles are locations of earthquakes with magnitude  $\geq 4$  and depth  $\leq 40$  km between 1977 and 2004. The map combines different datasets such as earthquake catalogue, active and presumed active faults, DEMs, shaded relief map, anaglyph images, and country shapefile to create a really realistic landscape visualization.

unit in the field. However, we have broadly estimated the slip rate by estimating the age of the displaced depositions, which appear to be from the Middle Pleistocene era. During the Late Pleistocene, the Spin Ghar fault in Sherzad District ( $34^{\circ}14'1.89''N$ ,

$69^{\circ}58'31.11''E$ ) has displaced a prominent alluvial fan by  $600 \pm 70$  m (e.g., Figure 9a-b). The fan is similar in morphology to one offset ( $800 \pm 70$  m) dated as  $172.0 \pm 16.4$  and  $218.7 \pm 21.1$  ka by Shnizai *et al.* (2020) on the Chaman fault based on Beryllium-10 cosmogenic



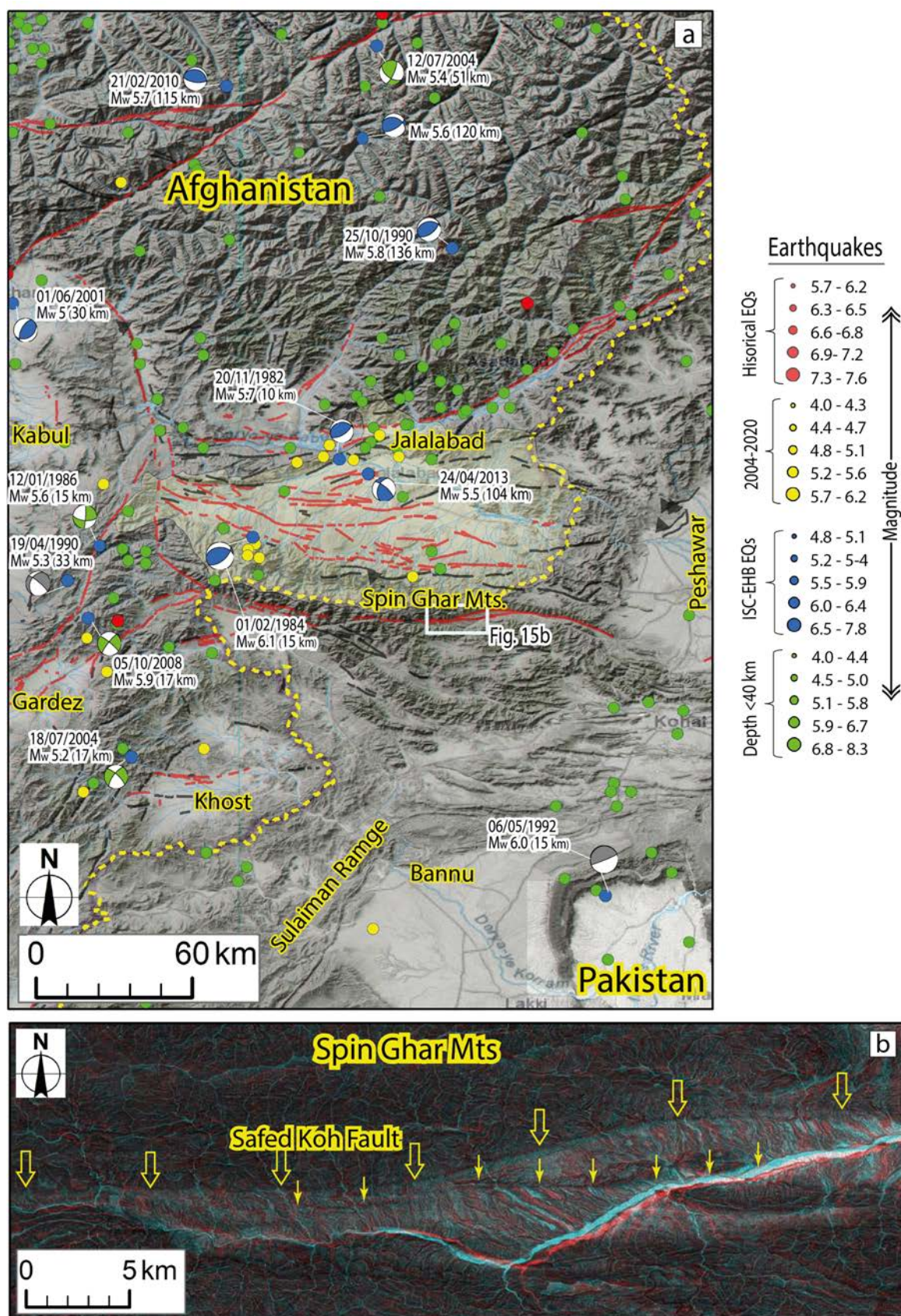


**Figure 15 – a)** Shaded relief topographic map of the Jalalabad Basin and the surrounding region. The earthquake locations are from the Global CMT catalogue (<https://www.globalcmt.org/CMTsearch.html>, Ekström *et al.*, 2012). The focal mechanisms show east-west striking thrust faults that are active in the Jalalabad Basin and Spin Ghar Mountains. This indicates that the ongoing displacement of the Indian plate with respect to Eurasia is accommodated by deformation in eastern Afghanistan. The focal mechanisms also show strike-slip faulting along the Gardez fault west of the basin. Shallow activity seems to be associated with the Sarobi, Konar, Safed Koh and Spin Ghar faults. **b)** Anaglyph image showing geomorphic expression of the Safed Koh fault along the southern margin of the Spin Ghar Mountains. The figure location is shown in Figure 6.



dating (see Figure 1b for location). The dated fan is located in Sayed Abad District of Wardak Province (33°48'48.49"N, 68°36'13.32"E), 135 km apart in a similar climatic setting with less than one-degree (25.2') difference in latitude. If we assume the fan offset by the Spin Ghar fault is between 172 ka and 218 ka, we can infer that the slip rate of the sinistral movement is between 2.7-3.5 mm/yr. According to *Abdullah et al. (2008)*, the Jalalabad Basin is filled with red to variegated continental deposits from the Neogene-Quaternary period, along with fine and coarse terrigenous materials (Figure 5). It also contains a small amount of lacustrine limestones and marls. *Ruleman et al. (2007)* also broadly estimated that the slip rate for the Spin Ghar fault ranges at 1-10 mm/yr based on the geological displacement of specific landforms in the Quaternary period. This provides general information about the continuity and expression of the fault. Without knowing the absolute age of the offset alluvial fan, it is impossible to verify the actual slip rates.

## 6 Conclusions

The plate boundary between Indian and Eurasian plates causes deformation in the east and north-eastern Afghanistan, which includes both north-south left-lateral faults, and east-west reverse and right-lateral faults. The boundary is not a single discrete fault but instead a broad zone of active faulting. These active faults in eastern Afghanistan have uplifted the Hindu Kush and Pamir Mountains, creating wide belts of low-elevation mountainous terrain intertwined with fault-bounded low-relief sedimentary basins. The Spin Ghar fault system is one of the major faults that lies north of the plate boundary and separates the Jalalabad Basin to the north from the east-west Spin Ghar Mountains to the south. We have made detailed active fault map using Landsat 8 satellite data and anaglyph images derived from the 1-arcsecond SRTM digital elevation model.

- For geological mapping, a suit of enhancing techniques has been applied to Landsat-8 data such as true colour composite (TCC), FCC, Band Ratios and PCA. The combination of these methods influences the quality and amount of the extracted information and highlights geological formations.
- We also used 3D anaglyph image to map active faults and recognise the area distribution of the exposed rocks and the density of structural formations.
- Our study shows that the Spin Ghar active fault strands across the basin can be recognized on the basis of geology and topography. The fault system contains multiple strands, which strike parallel to the Spin Ghar Ridge.
- Many deformed surfaces of Neogene-Quaternary age are observed along the Spin Ghar fault strands.

East-west and southwest-northeast-trending oblique-slip faults predominate in the area, which we infer to accommodate regional north-south left-lateral shearing by bookshelf faulting. The geomorphic features show that the fault continuously extends along the basin and mountain foot to the eastern border with Khyber-Pakhtunkhwa. West dipping reverse faults were also identified in bedrock terrain that may represent slip partitioning along the Spin Ghar fault system. The present study indicates that the mapped faults are active and the exhumed geological structures may be related to recent faulting. This research work provides a basis for further tectonics and hazard-related studies. However, further detailed field studies are needed in order to quantitatively evaluate the rates of active deformation in eastern Afghanistan.

## Acknowledgements

We would like to express our profound gratitude to Cara (Council for At-Risk Academics), IIE-SRF (Institute of International Education's Scholar Rescue Fund), and St. Johns College University of Oxford for supporting Zakeria Shnizai through a post-doctoral fellowship. We thank the Leverhulme Trust for support through the program EROICA (the Earthquake Ruptures of Iran and Central Asia, RPG-2018-371), and the NERC-funded COMET (GA/13/M/031). The authors are grateful to Prof. Takashi Nakata for creating anaglyph images from the 1-arcsecond SRTM DEM. We are also very grateful to Associate Editor Hongdan Deng and two anonymous reviewers for their helpful suggestions and comments that really helped the overall quality of the manuscript. We also thank the executive editor Robin Lacassin and the technical editor Mohamed Gouiza for the editorial handling.

## Author contributions

**Z. Shnizai** designed the project, collected the data, helped with data analysis and interpretation, and wrote the manuscript. **R. Walker** contributed to the manuscript design, data analysis and interpretation, proofread and made critical revisions to the manuscript.

## Data availability

The data used in this research is public and available from <https://earthexplorer.usgs.gov/>.

## Competing interests

The authors declare no competing interests.

## Peer review

This publication was peer-reviewed by Marie-Luce Chevalier and Jérôme Van der Woerd. The

full peer-review report can be found here: [tektonika.online/index.php/home/article/view/49/84](https://tektonika.online/index.php/home/article/view/49/84)

## Copyright notice

© Author(s) 2024. This article is distributed under the [Creative Commons Attribution 4.0 International License](https://creativecommons.org/licenses/by/4.0/), which permits unrestricted use, distribution, and reproduction in any medium, provided the original author(s) and source are credited, and any changes made are indicated.

## References

- Abdelaziz, R., Y. Abd El-Rahman, and S. Wilhelm (2018), Landsat-8 data for chromite prospecting in the Logar Massif, Afghanistan, *Heliyon*, 4(2), e00542, doi: [10.1016/j.heliyon.2018.e00542](https://doi.org/10.1016/j.heliyon.2018.e00542).
- Abdullah, S., and V. M. Chmyriov (1977), Map of mineral resources of afghanistan: Kabul.
- Abdullah, S., V. M. Chmyriov, and V. I. Dronov (2008), *Geology and Mineral Resources of Afghanistan*, 1–488 pp., British Geological Survey, London.
- Adiri, Z., R. Lhissou, A. El Harti, A. Jellouli, and M. Chakouri (2020), Recent advances in the use of public domain satellite imagery for mineral exploration: A review of landsat-8 and sentinel-2 applications, *Ore Geology Reviews*, 117, 103332, doi: [10.1016/j.oregeorev.2020.103332](https://doi.org/10.1016/j.oregeorev.2020.103332).
- Afghanistan Geological Survey (1996), Geological Map of Afghanistan.
- Aitchison, J. C., J. R. Ali, and A. M. Davis (2007), When and where did India and Asia collide?, *Journal of geophysical research*, 112(B5), 5423, doi: [10.1029/2006jb004706](https://doi.org/10.1029/2006jb004706).
- Ambraseys, N., and R. Bilham (2003), Earthquakes in Afghanistan, *Seismological Research Letters*, 74(2), 107–123, doi: [10.1785/gssrl.74.2.107](https://doi.org/10.1785/gssrl.74.2.107).
- Ambraseys, N., and R. Bilham (2014), The tectonic setting of bamiyan and seismicity in and near afghanistan for the past twelve centuries, in *After the Destruction of Giant Buddha Statues in Bamiyan (Afghanistan) in 2001: A UNESCO's Emergency Activity for the Recovering and Rehabilitation of Cliff and Niches*, edited by C. Margottini, pp. 101–152, Springer Berlin Heidelberg, Berlin, Heidelberg, doi: [10.1007/978-3-642-30051-6\\_6](https://doi.org/10.1007/978-3-642-30051-6_6).
- Azizi, H., M. A. Tarverdi, and A. Akbarpour (2010), Extraction of hydrothermal alterations from ASTER SWIR data from east Zanjan, northern Iran, *Advances in space research: the official journal of the Committee on Space Research*, 46(1), 99–109, doi: [10.1016/j.asr.2010.03.014](https://doi.org/10.1016/j.asr.2010.03.014).
- Beun, N., P. Bordet, and J. P. Carbonnel (1979), Premières données quantitative relatives au coulissage du décrochement de Chaman (Afghanistan du sud-est), *Comptes rendus de l'Académie des Sciences*, 288, 931–934.
- Crupa, W. E., S. D. Khan, J. Huang, A. S. Khan, and A. Kasi (2017), Active tectonic deformation of the western Indian plate boundary: A case study from the Chaman Fault System, *Journal of Asian Earth Sciences*, 147, 452–468, doi: [10.1016/j.jseaes.2017.08.006](https://doi.org/10.1016/j.jseaes.2017.08.006).
- Dalaisson, M., R. Jolivet, E. M. van Rijsingen, and S. Michel (2021), The interplay between seismic and aseismic slip along the chaman fault illuminated by InSAR, *Journal of Geophysical Research, [Solid Earth]*, 126(12), 1–23, doi: [10.1029/2021jb021935](https://doi.org/10.1029/2021jb021935).
- Denikaev, S. S., V. P. Feoktistov, I. V. Pyzhyanov, A. A. Adjuruddin, S. N. Narbaev, and Y. M. Konev (1971), Geology and minerals in the south part of Eastern Afghanistan (Report of the Kabul team on the work in 1970), *Tech. rep.*, Kabul, Rec. Off. DGMS, Kabul.
- Dewey, J. W. (2006), Seismicity of Afghanistan and vicinity, *Tech. Rep. No.28*, U.S. Geological Survey, doi: [10.3133/ofr20061185](https://doi.org/10.3133/ofr20061185).
- Dhakal, S. (2015), Evolution of Geomorphologic Hazards in Hindu Kush Himalaya, in *Mountain Hazards and Disaster Risk Reduction*, edited by H. K. Nibanupudi and R. Shaw, 1 ed., pp. 53–72, Springer Japan, Tokyo, doi: [10.1007/978-4-431-55242-0\\_4](https://doi.org/10.1007/978-4-431-55242-0_4).
- Doebrich, J. L., R. R. Wahl, S. D. Ludington, P. G. Chirico, C. J. Wandrey, R. G. Bohannon, G. J. Orris, J. D. Bliss, A. Wasy, and M. O. Younsi (2006), Geologic and mineral resource map of Afghanistan, *Tech. Rep. No.2006-10*, U.S. Geological Survey, doi: [10.3133/ofr20061038](https://doi.org/10.3133/ofr20061038).
- Ekström, G., M. Nettles, and A. M. Dziewoński (2012), The global CMT project 2004–2010: Centroid-moment tensors for 13,017 earthquakes, *Physics of the Earth and Planetary Interiors*, 200–201, 1–9, doi: [10.1016/j.pepi.2012.04.002](https://doi.org/10.1016/j.pepi.2012.04.002).
- Ghrefat, H., A. Y. Kahal, K. Abdelrahman, H. J. Alfaifi, and S. Qaysi (2021), Utilization of multispectral landsat-8 remote sensing data for lithological mapping of southwestern Saudi Arabia, *Journal of King Saud University - Science*, 33(4), 101414, doi: [10.1016/j.jksus.2021.101414](https://doi.org/10.1016/j.jksus.2021.101414).
- Grebby, S., D. Cunningham, K. Tansey, and J. Naden (2014), The impact of vegetation on lithological mapping using airborne multispectral data: A case study for the north troodos region, cyprus, *Remote Sensing*, 6(11), 10860–10887, doi: [10.3390/rs61110860](https://doi.org/10.3390/rs61110860).
- Hashim, M., S. Ahmad, M. A. Johari, and A. B. Pour (2013), Automatic lineament extraction in a heavily vegetated region using Landsat Enhanced Thematic Mapper (ETM+) imagery, *Advances in space research: the official journal of the Committee on Space Research*, 51(5), 874–890, doi: [10.1016/j.asr.2012.10.004](https://doi.org/10.1016/j.asr.2012.10.004).
- Inzana, J., T. Kusky, G. Higgs, and R. Tucker (2003), Supervised classifications of Landsat TM band ratio images and Landsat TM band ratio image with radar for geological interpretations of central Madagascar, *Journal of African Earth Sciences*, 37(1), 59–72, doi: [10.1016/S0899-5362\(03\)00071-X](https://doi.org/10.1016/S0899-5362(03)00071-X).
- ISC-EHB (2023), ISC-EHB dataset, doi: [10.31905/PY08W6S3](https://doi.org/10.31905/PY08W6S3).
- Lawrence, R. D., S. H. Khan, and T. Nakata (1992), Chaman Fault, Pakistan-Afghanistan, *Annales Tectonicae*, 6, 196–223.
- Leleu, S., J.-F. Ghienne, and G. Manatschal (2009), Alluvial fan development and morpho-tectonic evolution in response to contractional fault reactivation (late Cretaceous-Palaeocene), provence, france, *Basin Research*, 21(2), 157–187, doi: [10.1111/j.1365-2117.2008.00378.x](https://doi.org/10.1111/j.1365-2117.2008.00378.x).
- Mcdougall, J. W., and A. Hu (1991), Fold and thrust propagation in the western himalaya based on a balanced cross section of the surghar range and kohat plateau, pakistan (1), *AAPG bulletin*, 75(3), 463–478, doi: [10.1306/0c9b280d-1710-11d7-8645000102c1865d](https://doi.org/10.1306/0c9b280d-1710-11d7-8645000102c1865d).
- Mohadjer, S., R. Bendick, A. Ischuk, S. Kuzikov, A. Kostuk,



- U. Saydullaev, S. Lodi, D. M. Kakar, A. Wasy, M. A. Khan, P. Molnar, R. Bilham, and A. V. Zubovich (2010), Partitioning of India-Eurasia convergence in the Pamir-Hindu kush from GPS measurements, *Geophysical research letters*, 37(4), 1–6, doi: 10.1029/2009gl041737.
- MUDA (2015), State of Afghan Cities 2015 (Volume 1), *Tech. rep.*, Ministry of Urban Development Affairs, Independent Directorate of Local Governance, Kabul Municipality.
- Nakata, T., H. Tsutsumi, S. H. Khan, and R. D. Lawrence (1991), Active faults of Pakistan: map sheets and inventories (Special Publication), *Research Center for Regional Geography, Hiroshima University*, 21, 141.
- Prevot, R., D. Hatzfeld, S. W. Roecker, and P. Molnar (1980), Shallow earthquakes and active tectonics in eastern Afghanistan, *Journal of Geophysical Research, [Solid Earth]*, 85(B3), 1347–1357, doi: 10.1029/JB085iB03p01347.
- Quittmeyer, R. C., and K. H. Jacob (1979), Historical and modern seismicity of pakistan, afghanistan, northwestern india, and southeastern iran, *Bulletin of the Seismological Society of America*, 69(3), 773–823.
- Ruleman, C. A., A. J. Crone, M. N. Machette, K. M. Haller, and K. S. Rukstales (2007), Map and database of probable and possible quaternary faults in afghanistan, *Tech. rep.*, U.S. Geological Survey, doi: 10.3133/ofr20071103.
- Shareq, A. (1981), Geological observations and geophysical investigations carried out in afghanistan over the period of 1972–1979, in *Zagros, Hindu Kush, Himalaya: Geodynamic Evolution*, vol. 3, edited by H. K. Gupta and F. M. Delany, pp. 75–86, American Geophysical Union, Washington, D. C., doi: 10.1029/gd003p0075.
- Shareq, A. (1993), Seismic hazard assessment in the Islamic state of Afghanistan, in *The practice of earthquake hazard assessment*, edited by R. K. McGuire, pp. 1–6, International Association of Seismology and Physics of the Earth's Interior.
- Shnizai, Z. (2020a), Mapping of active and presumed active faults in Afghanistan by interpretation of 1-arcsecond SRTM anaglyph images, *Journal of Seismology*, 24(6), 1131–1157, doi: 10.1007/s10950-020-09933-4.
- Shnizai, Z. (2020b), Active Tectonics and Seismic Hazard Assessment of Afghanistan and Slip-rate Estimation of the Chaman Fault Based on Cosmogenic <sup>10</sup>Be Dating, Ph.D. thesis, Doshisha University, doi: 10.14988/00027636.
- Shnizai, Z., and H. Tsutsumi (2020), Active Faults and Seismic Hazard in the Kabul Basin, Afghanistan, *The Harris Science Research Institute of Doshisha University*, 61(2), 96–107, doi: 10.14988/00027353.
- Shnizai, Z., Y. Matsushi, and H. Tsutsumi (2020), Late Pleistocene slip rate of the Chaman fault based on <sup>10</sup>Be exposure dating of offset geomorphic surfaces near Kabul, Afghanistan, *Tectonophysics*, 795, 228,593, doi: 10.1016/j.tecto.2020.228593.
- Shnizai, Z., M. Talebian, S. Valkanotis, and R. Walker (2022), Multiple factors make Afghan communities vulnerable to earthquakes, *Temblor*, doi: 10.32858/temblor.266.
- Shnizai, Z., R. Walker, and H. Tsutsumi (2024), The Chaman and Paghman active faults, west of Kabul, Afghanistan: Active tectonics, geomorphology, and evidence for rupture in the destructive 1505 earthquake, *Journal of Asian Earth Sciences*, 259, 105,925, doi: 10.1016/j.jseaes.2023.105925.
- Shroder, J. F., N. Eqrar, H. Waizy, H. Ahmadi, and B. J. Weihs (2022), Review of the Geology of Afghanistan and its water resources, *International geology review*, 64(7), 1009–1031, doi: 10.1080/00206814.2021.1904297.
- Siehl, A. (2017), Structural setting and evolution of the afghan orogenic segment – a review, *Geological Society, London, Special Publications*, 427(1), 57–88, doi: 10.1144/SP427.8.
- Szeliga, W., R. Bilham, D. M. Kakar, and S. H. Lodi (2012), Interseismic strain accumulation along the western boundary of the indian subcontinent, *Journal of Geophysical Research, [Solid Earth]*, 117(B8), doi: 10.1029/2011JB008822.
- Tapponnier, P., M. Mattauer, F. Proust, and C. Cassaigneau (1981), Mesozoic ophiolites, sutures, and large-scale tectonic movements in Afghanistan, *Earth and planetary science letters*, 52(2), 355–371, doi: 10.1016/0012-821X(81)90189-8.
- Treloar, P. J., and C. N. Izatt (1993), Tectonics of the himalayan collision between the indian plate and the afghan block: a synthesis, *Geological Society, London, Special Publications*, 74(1), 69–87, doi: 10.1144/GSL.SP.1993.074.01.06.
- Ul-Hadi, S., S. D. Khan, L. A. Owen, A. S. Khan, K. A. Hedrick, and M. W. Caffee (2013), Slip-rates along the Chaman fault: Implication for transient strain accumulation and strain partitioning along the western Indian plate margin, *Tectonophysics*, 608, 389–400, doi: 10.1016/j.tecto.2013.09.009.
- USGS (2023), Earthquake Catalog, <https://earthquake.usgs.gov/earthquakes/search/>, accessed: 2022-11-4.
- Wheeler, R. L., C. G. Bufe, M. L. Johnson, R. L. Dart, and G. A. Norton (2005), Seismotectonic map of Afghanistan, with annotated bibliography, *Tech. Rep. 2005–1264*, U.S. Geological Survey.
- Yang, Z., P. Willis, and R. Mueller (2008), Impact of Band-Ratio Enhanced AWiFS Image to Crop Classification Accuracy, *Proceeding Pecora 17*, 17(1).
- Yeats, R. S., R. D. Lawrence, S. Jamil-ud din, and S. H. Khan (1979), Surface effects of the March 16 1978 earthquake, Pakistan-Afghanistan border, in *Geodynamics of Pakistan*, edited by A. Farah; and K. A. DeJong, pp. 359–361, Geological Survey of Pakistan, Quetta.